Table 5. Flow of Supplemental Oxygen Required Before and After Starting Epoprostenol Therapy

Patient no.	Baseline	Best	Later
1	3	2	9
2	2	5	8
3	3	2	15
4	4	4	10
5	2	3	12
6	NA	3	10
7	3	3	12
8	3	4	10
P value		NS	<0.01

Data indicate the flow of supplemental oxygen (L/min).
Repeated-measures analysis of variance with Bonferroni correction was performed. P values indicate "best" and "later" values compared with the "baseline" value.
Baseline, before starting epoprostenol therapy; best, at the time when patients achieved the best values for cardiac index; later, maximum oxygen flow required while the dose of epoprostenol was increased later.

index was obtained at 164.1±79.7 days after initiation of epoprostenol with a dose of 24.4±5.6 ng·kg^{-1}·min^{-1}.

After the application of epoprostenol, the WHO functional class improved at least temporarily to class II or III in all patients. The mean 6-min walk distance significantly increased from 97.5±39.2 to 329.4±34.6 m (P<0.001) (Table 2; Figure 2A). As mentioned above, plasma levels of BNP were not always elevated at baseline. In patients who had high BNP levels prior to epoprostenol therapy, BNP levels were significantly reduced after therapy. In total, the mean BNP levels were significantly reduced from 381.3±136.8 to 55.2±14.4 pg/ml (P<0.05). The mean cardiac index significantly improved from 2.1±0.1 to 2.9±0.3 L·min^{-1}·m^{-2} (P<0.05). However, the mean PAP and right atrial pressure did not change between before and after epoprostenol therapy. Although mixed venous oxygen saturation was increased and pulmonary vascular resistance was decreased after epoprostenol therapy, these differences were not statistically significant.

Associated Therapy

Associated therapy before and after epoprostenol therapy is shown in Tables 2 and 3. At baseline, anticoagulation and diuretics were used in all patients, digitalis was given in 4 patients (patients 2, 5, 6, and 7), and no calcium channel blockers were used in any of these patients. An endothelin receptor antagonist, bosentan, was used in 2 patients (patient 7: 125 mg/day; patient 8: 250 mg/day) and a phosphodiesterase 5 inhibitor, sildenafil, was used in 2 patients (patient 3: 60 mg/day; patient 7: 40 mg/day). The doses of bosentan and sildenafil were unchanged during epoprostenol therapy. Catecholamines were not used at the time when patients achieved the best values for the cardiac index. Anticoagulation was discontinued in 2 patients (patients 3 and 4) based on our previous report regarding the risk of alveolar hemorrhage induced by concomitant use with epoprostenol.[13] Digitalis was stopped in patient 5 who manifested bradycardia. All other medications were unchanged after epoprostenol therapy.

Radiographic Changes and Oxygen Supplementation During Epoprostenol Therapy

All 8 patients manifested atypical radiographic features as IPAH at baseline (Table 4; Figure 3). Their chest radiographs revealed not only dilated pulmonary arteries and enlargement of the heart, but also peripheral interstitial infiltrates in both lung fields, and sometimes prominent septal lines. High-resolution CT scans showed pleural effusion, thickened interlobular septa, bilateral ground-glass opacities, and a mosaic pattern of lung attenuation. Lymphadenopathy in the mediastinum, which is sometimes observed as a reactive adenopathy in PVOD, was detected in 1 patient with PVOD and 2 patients with PCH. After initiation of epoprostenol therapy, all patients' chest X-rays or CTs showed thickened interlobular and intralobular septae and an increased density of interstitial opacities. Three of them also showed an increase in pleural effusion. At that time, we temporarily stopped increasing the dose of epoprostenol and added diuretics and/or intravenous infusion of catecholamines. After congestion improved, we started to titrate the dosage of epoprostenol again.

Before epoprostenol therapy, patients required oxygen supplementation with 2.9±0.3 L/min (Table 5). At the time when patients achieved the best values for cardiac index, patients needed 3.3±0.4 L/min of supplemental oxygen. As the dose of epoprostenol was increased, patients showed deterioration of oxygen desaturation and an increase in interstitial infiltrates on chest X-rays. They finally needed an oxygen supplement at a significantly higher flow (10.8±0.8 L/min) than they did before epoprostenol therapy (P<0.01).

Discussion

Among a variety of diseases that can lead to pulmonary hypertension, PVOD and PCH are especially rare, and their classification has been changed at all the World Symposiums on Pulmonary Hypertension. In the previous classification of pulmonary hypertension, they were categorized in a subgroup of pulmonary arterial hypertension, termed "pulmonary arterial hypertension associated with significant venous or capillary involvement".[2] In the most recent Dana Point classification, these diseases are classified as Group 1', similar to but with some differences from Group 1, because of their similarities in histological changes, clinical presentations, risk factors and having shared mutations in the BMPR2 gene, similar to that for IPAH.[3]

The prognosis of PVOD and PCH is still unknown because of the rareness of the disease. It is believed to be poor, with most patients with PVOD dying within 2 years from the initial presentation.[7] Most PCH patients rapidly progress to death over several months of the clinical disease.[14] In the last decade, PAH-targeted drugs have improved the survival of patients with PAH.[6,15,16] However, no medical treatment has been proven to improve the survival of patients with PVOD and PCH. Therefore, patients with PVOD and PCH have a higher mortality and a lower chance of survival compared with patients with IPAH.

Currently, lung transplantation is the only method to cure these diseases and patients who desire it are placed on the list for lung transplantation as soon as possible.[4] However, there are few organ donors available to undergo cadaveric lung transplantation. In Japan, where organ transplantation has been recently introduced, chances of transplantation are very limited and the mean waiting time for lung transplantation is reported to be approximately 3 years. In most cases, it is difficult for patients to survive for this long period of time considering their poor prognosis. Although LDLLT is expected to be an alternative for cadaveric lung transplantation, there are more strict criteria for donors of LDLLT.[17,18] Not all patients and their families who desire to receive lung transplantation can

undergo LDLLT. A therapeutic option is required for patients waiting for a suitable donor or for those who are not candidates for lung transplantation.

Continuous intravenous infusion of epoprostenol has been reported to improve the prognosis of IPAH.[6,19] However, its indication for PVOD and PCH is still controversial. Some reports have cautioned against the possibility of causing massive pulmonary edema by application of epoprostenol for patients with PVOD or PCH.[9,10] Application of epoprostenol for PVOD or PCH might be unsuccessful because when the pulmonary arterioles dilate and resistance of the pulmonary veins remains fixed, transcapillary hydrostatic pressure might increase and pulmonary edema might occur.[20] In contrast, some patients with PVOD have been reported to show temporary amelioration by application of epoprostenol.[7,8] There is 1 case report that showed that long-term epoprostenol therapy improved exercise capacity and pulmonary hemodynamics in PVOD.[8] The authors concluded that in this case, the administration of epoprostenol played a role in the regulation of vascular tone in pulmonary venules rather than in the pulmonary arteries. Detailed hemodynamic measurements showed that microvascular pressures initially increased during an infusion of no more than $6\,ng \cdot kg^{-1} \cdot min^{-1}$ of epoprostenol, but at higher doses, cardiac output increased and the calculated pulmonary vascular resistance decreased.[21] To the best of our knowledge, there are no reports that have described patients with PCH being successfully treated with epoprostenol.

We administered epoprostenol to 8 patients with PVOD or PCH because they had no other therapeutic option besides lung transplantation. In our cases, we cautiously administered epoprostenol, starting with a low dose. When we increased the dose of epoprostenol too quickly, an imbalance of dilatation between pulmonary arterioles and veins occurred. However, if we slowly increased the dose in a step-wise manner and used diuretics or inotropes as necessary, the transcapillary hydrostatic pressure decreased and we could avoid severe pulmonary congestion.

For the successful treatment of PVOD and PCH with epoprostenol, early recognition and diagnosis of PVOD/PCH are essential in addition to the careful application of epoprostenol. A lung biopsy is the only method of definitively diagnosing PVOD and PCH. However, in most cases, it is difficult to perform a lung biopsy because of the severity of the patients' condition. This is why it is important to clinically diagnose PVOD/PCH with available data and results of examinations. It is vital to be aware of poor oxygenation, low DLco, and distinct radiographic findings to diagnose or suspect PVOD and PCH.[20,22] In the present study, all patients presented with marked oxygen desaturation on exertion and a severe decrease in DLco. Their chest radiographs and high-resolution CT scans revealed radiographic findings that were characteristic for PVOD and PCH, but not IPAH (Table 4; Figure 3).[14,23] Early recognition of PVOD/PCH in patients with pulmonary hypertension is possible based on these clinical and radiographic characteristics. This might lead to careful introduction and dose adjustment of epoprostenol and to successful treatment of these complicated diseases.

The present study showed that as a result of epoprostenol therapy, clinical and hemodynamic data were improved (Table 2; Figure 2), at least temporarily. All patients were critically ill before starting epoprostenol therapy. The mean 6-min walk distance, which is reported to correlate well with the prognosis in IPAH, was significantly increased after therapy. Our data showed that epoprostenol significantly improved exercise capacity and increased cardiac output of patients with PVOD or PCH, but did not decrease PAP and right atrial pressure, which are known to determine the survival of IPAH.[24] This might be one of the reasons why patients eventually showed deterioration. Most patients showed maximal improvement within half a year after starting epoprostenol therapy. In some cases, with cautious control of epoprostenol therapy, there is a possibility of longer survival than previously reported. The dose of epoprostenol given at the time when patients showed maximal improvement in clinical status was $24\,ng \cdot kg^{-1} \cdot min^{-1}$, regardless of whether they could undergo LDLLT. Although they could walk further in the 6-min walk test because of increased cardiac output with epoprostenol therapy, patients showed deterioration of interstitial infiltration in chest X-rays and CT scans and needed a higher flow of supplemental oxygen. Considering severe oxygen desaturation and limited prognosis with epoprostenol therapy, further studies are required to determine better therapeutic strategies to treat PVOD and PCH.

Conclusions

We applied epoprostenol treatment to 8 patients with atypical clinical and radiographic findings such as IPAH. Histological findings revealed that 6 patients had PVOD and the other 2 patients had PCH. Epoprostenol was applied at a higher dose and for a longer period than previously reported cases, and worked as a bridge to lung transplantation for 4 patients. It was also applied in 4 patients who had no chance to undergo lung transplantation. All patients showed temporary amelioration in WHO functional class, exercise capacity, and cardiac index with long-term epoprostenol therapy. When patients are suspected of having PVOD or PCH by characteristic clinical and radiographic findings, careful application of epoprostenol can be considered as a bridge to lung transplantation or as the only method to improve their clinical condition because they have no other therapeutic options.

References

1. Fishman AP. Clinical classification of pulmonary hypertension. *Clin Chest Med* 2001; **22:** 385–391, vii.
2. Simonneau G, Galie N, Rubin LJ, Langleben D, Seeger W, Domenighetti G, et al. Clinical classification of pulmonary hypertension. *J Am Coll Cardiol* 2004; **43:** 5S–12S.
3. Simonneau G, Robbins IM, Beghetti M, Channick RN, Delcroix M, Denton CP, et al. Updated clinical classification of pulmonary hypertension. *J Am Coll Cardiol* 2009; **54:** S43–S54.
4. McLaughlin VV, Archer SL, Badesch DB, Barst RJ, Farber HW, Lindner JR, et al. ACCF/AHA 2009 Expert Consensus Document on Pulmonary Hypertension: A report of the American College of Cardiology Foundation Task Force on Expert Consensus Documents and the American Heart Association: Developed in collaboration with the American College of Chest Physicians, American Thoracic Society, Inc., and the Pulmonary Hypertension Association. *Circulation* 2009; **119:** 2250–2294.
5. Higenbottam T, Butt AY, McMahon A, Westerbeck R, Sharples L. Long-term intravenous prostaglandin (epoprostenol or iloprost) for treatment of severe pulmonary hypertension. *Heart* 1998; **80:** 151–155.
6. Barst RJ, Rubin LJ, Long WA, McGoon MD, Rich S, Badesch DB, et al. A comparison of continuous intravenous epoprostenol (prostacyclin) with conventional therapy for primary pulmonary hypertension: The primary pulmonary hypertension study group. *N Engl J Med* 1996; **334:** 296–302.
7. Holcomb BW Jr, Loyd JE, Ely EW, Johnson J, Robbins IM. Pulmonary veno-occlusive disease: A case series and new observations. *Chest* 2000; **118:** 1671–1679.
8. Okumura H, Nagaya N, Kyotani S, Sakamaki F, Nakanishi N, Fukuhara S, et al. Effects of continuous IV prostacyclin in a patient with pulmonary veno-occlusive disease. *Chest* 2002; **122:** 1096–1098.
9. Palmer SM, Robinson LJ, Wang A, Gossage JR, Bashore T, Tapson VF. Massive pulmonary edema and death after prostacyclin infusion

in a patient with pulmonary veno-occlusive disease. *Chest* 1998; **113:** 237–240.
10. Humbert M, Maitre S, Capron F, Rain B, Musset D, Simonneau G. Pulmonary edema complicating continuous intravenous prostacyclin in pulmonary capillary hemangiomatosis. *Am J Respir Crit Care Med* 1998; **157:** 1681–1685.
11. Montani D, Jais X, Price LC, Achouh L, Degano B, Mercier O, et al. Cautious epoprostenol therapy is a safe bridge to lung transplantation in pulmonary veno-occlusive disease. *Eur Respir J* 2009; **34:** 1348–1356.
12. Barst RJ, McGoon M, Torbicki A, Sitbon O, Krowka MJ, Olschewski H, et al. Diagnosis and differential assessment of pulmonary arterial hypertension. *J Am Coll Cardiol* 2004; **43:** 40S–47S.
13. Ogawa A, Matsubara H, Fujio H, Miyaji K, Nakamura K, Morita H, et al. Risk of alveolar hemorrhage in patients with primary pulmonary hypertension: Anticoagulation and epoprostenol therapy. *Circ J* 2005; **69:** 216–220.
14. Almagro P, Julia J, Sanjaume M, Gonzalez G, Casalots J, Heredia JL, et al. Pulmonary capillary hemangiomatosis associated with primary pulmonary hypertension: Report of 2 new cases and review of 35 cases from the literature. *Medicine (Baltimore)* 2002; **81:** 417–424.
15. Fukumoto Y, Shimokawa H. Recent progress in the management of pulmonary hypertension. *Circ J* 2011; **75:** 1801–1810.
16. Humbert M, Sitbon O, Chaouat A, Bertocchi M, Habib G, Gressin V, et al. Survival in patients with idiopathic, familial, and anorexigen-associated pulmonary arterial hypertension in the modern management era. *Circulation* 2010; **122:** 156–163.
17. Starnes VA, Bowdish ME, Woo MS, Barbers RG, Schenkel FA, Horn MV, et al. A decade of living lobar lung transplantation: Recipient outcomes. *J Thorac Cardiovasc Surg* 2004; **127:** 114–122.
18. Date H, Kusano KF, Matsubara H, Ogawa A, Fujio H, Miyaji K, et al. Living-donor lobar lung transplantation for pulmonary arterial hypertension after failure of epoprostenol therapy. *J Am Coll Cardiol* 2007; **50:** 523–527.
19. Akagi S, Nakamura K, Miyaji K, Ogawa A, Kusano KF, Ito H, et al. Marked hemodynamic improvements by high-dose epoprostenol therapy in patients with idiopathic pulmonary arterial hypertension. *Circ J* 2010; **74:** 2200–2205.
20. Mandel J, Mark EJ, Hales CA. Pulmonary veno-occlusive disease. *Am J Respir Crit Care Med* 2000; **162:** 1964–1973.
21. Davis LL, deBoisblanc BP, Glynn CE, Ramirez C, Summer WR. Effect of prostacyclin on microvascular pressures in a patient with pulmonary veno-occlusive disease. *Chest* 1995; **108:** 1754–1756.
22. Frazier AA, Franks TJ, Mohammed TL, Ozbudak IH, Galvin JR. From the archives of the AFIP: Pulmonary veno-occlusive disease and pulmonary capillary hemangiomatosis. *Radiographics* 2007; **27:** 867–882.
23. Resten A, Maitre S, Humbert M, Rabiller A, Sitbon O, Capron F, et al. Pulmonary hypertension: CT of the chest in pulmonary venoocclusive disease. *AJR Am J Roentgenol* 2004; **183:** 65–70.
24. D'Alonzo GE, Barst RJ, Ayres SM, Bergofsky EH, Brundage BH, Detre KM, et al. Survival in patients with primary pulmonary hypertension: Results from a national prospective registry. *Ann Intern Med* 1991; **115:** 343–349.

Circulation Journal
Official Journal of the Japanese Circulation Society
http://www.j-circ.or.jp

ORIGINAL ARTICLE
Imaging

Normal Values of Real-Time 3-Dimensional Echocardiographic Parameters in a Healthy Japanese Population

– The JAMP-3D Study –

Shota Fukuda, MD; Hiroyuki Watanabe, MD; Masao Daimon, MD; Yukio Abe, MD; Akihiro Hirashiki, MD; Kumiko Hirata, MD; Hiroshi Ito, MD; Masumi Iwai-Takano, MD; Katsuomi Iwakura, MD; Chisato Izumi, MD; Takayuki Hidaka, MD; Toshinori Yuasa, MD; Kazuya Murata, MD; Satoshi Nakatani, MD; Kazuaki Negishi, MD; Kazuhiro Nishigami, MD; Tomoko Nishikage, BSc; Takahiro Ota, MD; Akihiro Hayashida, MD; Konomi Sakata, MD; Nobuhiro Tanaka, MD; Satoshi Yamada, MD; Kazuhiro Yamamoto, MD; Junichi Yoshikawa, MD

Background: The recently developed real-time 3-dimensional echocardiography (RT3DE) is a promising imaging method to quantify cardiac chamber volumes and their functions in clinical practice. However, normal reference values of RT3DE parameters have not been fully investigated in a large, healthy Japanese population.

Methods and Results: This study consisted of 410 healthy subjects aged from 20 to 69 years who had a RT3DE at one of the 23 collaborating institutions. All subjects had no history of cardiac disease and no risk factors. The mean values in men and women were as follows: 50±12 ml/m^2 and 46±9 ml/m^2 for left ventricular (LV) end-diastolic volume index, 19±5 ml/m^2 and 17±4 ml/m^2 for end-systolic volume index, 61±4% and 63±4% for ejection fraction, 64±12 g/m^2 and 56±11 g/m^2 for mass index, 23±6 ml/m^2 and 24±6 ml/m^2 for left atrial (LA) maximum volume index, 10±3 ml/m^2 and 10±3 ml/m^2 for minimum volume index, and 58±6% and 58±6% for percent volume change. LV sizes decreased with age, whereas LV mass index did not change. LA sizes slightly increased with age.

Conclusions: This multicenter investigation determined normal reference values for LV and LA sizes, and their functional parameters on RT3DE in a large, healthy Japanese population. The results of the present study support the use of RT3DE for the diagnosis and management of cardiovascular disease. (*Circ J* 2012; **76:** 1177–1181)

Key Words: Echocardiography; Japanese; Population

Transthoracic echocardiography is the standard imaging modality for the assessment of cardiovascular anatomy, function and physiology in clinical practice.[1] The available normal reference values for echocardiographic measurements have been provided by the American Society of Echocardiography and European Association of Echocardiog-

Received November 1, 2011; revised manuscript received January 16, 2012; accepted January 17, 2012; released online February 24, 2012
Time for primary review: 14 days

Department of Medicine, Osaka Ekisaikai Hospital, Osaka (S.F.); Department of Cardiology, Sakakibara Heart Institute, Japan Research Promotion Society of Cardiovascular Disease, Tokyo (H.W.); Department of Cardiology, Juntendo University School of Medicine, Tokyo (M.D.); Department of Cardiology, Osaka City General Hospital, Osaka (Y.A.); Department of Cardiology, Nagoya University Hospital, Nagoya (A. Hirashiki); Department of Cardiology, Wakayama Medical University, Wakayama (K.H.); Department of Cardiovascular Medicine, Okayama University Graduate School of Medicine, Okayama (H.I.); Department of Infection Control and Laboratory Medicine, Fukushima Medical University, Fukushima (M.I.-T.); Division of Cardiology, Sakurabashi Watanabe Hospital, Osaka (K.I.); Department of Cardiology, Tenri Hospital, Tenri (C.I.); Department of Cardiovascular Medicine, Hiroshima University Hospital, Hiroshima (T.H.); Department of Cardiovascular, Respiratory and Metabolic Medicine, Graduate School of Medicine, Kagoshima University, Kagoshima (T.Y.); Division of Laboratory, Yamaguchi University Hospital, Ube (K.M.); Department of Health Sciences, Osaka University Graduate School of Medicine, Suita (S.N.); Department of Medicine and Biological Science, Gunma University Graduate School of Medicine, Maebashi (K. Negishi); Department of Critical Care and Cardiology, Saiseikai Kumamoto Hospital, Kumamoto (K. Nishigami); Department of Physiological Laboratory, Osaka Seamen's Insurance Hospital, Osaka (T.N.); Division of Cardiology, Fuchu Hospital, Izumi (T.O.); Division of Cardiology, Kawasaki Medical School, Kurashiki (A. Hayashida); Second Department of Internal Medicine, Kyorin University School of Medicine, Mitaka (K.S.); Department of Cardiology, Tokyo Medical University, Tokyo (N.T.); Department of Cardiovascular Medicine, Hokkaido University Graduate School of Medicine, Sapporo (S.Y.); Department of Cardiovascular Medicine, Osaka University Graduate School of Medicine, Suita (K.Y.); and Nishinomiya Watanabe Cardiovascular Center, Nishinomiya (J.Y.), Japan
Mailing address: Shota Fukuda, MD, PhD, Department of Medicine, Osaka Ekisaikai Hospital, 2-1-10 Honden, Nishi-ku, Osaka 550-0022, Japan. E-mail: h-syouta@mve.biglobe.ne.jp

ISSN-1346-9843 doi:10.1253/circj.CJ-11-1256

All rights are reserved to the Japanese Circulation Society. For permissions, please e-mail: cj@j-circ.or.jp

Table 1. Clinical Characteristics of the Enrolled Subjects

Age (years)	Men						Women					
	Overall	20–29	30–39	40–49	50–59	60–69	Overall	20–29	30–39	40–49	50–59	60–69
n	253	55	67	51	41	39	157	41	34	30	28	24
Weight, kg	66±9	65±8	67±8	67±9	69±10	62±11	50±6*	50±5*	50±5*	52±5*	49±6*	50±7*
Height, cm	170±6	171±6	171±5	171±7	170±7	165±6	156±5*	157±5*	157±5*	158±6*	153±4*	153±6*
BSA, kg/m²	1.8±0.1	1.8±0.1	1.8±0.1	1.8±0.1	1.8±0.2	1.7±0.1	1.5±0.1*	1.5±0.1*	1.5±0.1*	1.5±0.1*	1.4±0.1*	1.5±0.1*
HR, beats/min	66±10	65±10	65±9	67±10	65±10	65±9	67±9	66±10	69±8	67±9	66±8	67±10
SBP, mmHg	121±10	117±10	121±10	123±10	122±10	125±10	115±12*	111±8*	113±11*	113±12*	121±14	123±13
DBP, mmHg	73±9	70±8	73±10	76±7	74±10	73±8	69±9	65±7*	68±8*	68±10*	73±11	72±9

Data are presented as mean±SD. *P<0.05 vs. the corresponding parameter in men.
BSA, body surface area; HR, heart rate; SBP, systolic blood pressure; DBP, diastolic blood pressure.

Table 2. Normal Values of LV Parameters

Age (years)	Men						Women					
	Overall	20–29	30–39	40–49	50–59	60–69	Overall	20–29	30–39	40–49	50–59	60–69
n	222	48	58	46	36	34	134	37	27	25	23	22
EDV, ml	86±22	98±22	93±19	90±19	82±22	73±18	67±14*	68±15*	67±9*	76±14*	63±11*	59±12*
ESV, ml	34±10	39±10	36±8	36±9	31±9	28±8	25±6*	25±6*	25±4*	29±6*	23±5*	22±6*
EDV/BSA, ml/m²	50±12	56±12	52±10	51±11	45±12	44±12	46±9*	46±9*	46±7*	50±9	44±8	41±8
ESV/BSA, ml/m²	19±5	22±6	20±4	20±5	17±5	17±5	17±4*	17±4*	17±3*	19±4	16±4	15±4
EF, %	61±4	61±3	62±3	61±4	63±3	61±5	63±4*	63±4*	62±4	63±3*	64±3	63±5
Mass, g	113±22	115±23	112±21	115±23	113±23	107±17	83±17*	81±16*	80±16*	90±20*	84±15*	80±16*
Mass/BSA, g/m²	64±12	66±12	63±12	64±12	64±13	64±10	56±11*	55±10*	55±11*	58±12	58±9	55±9*
MV ratio	1.3±0.3	1.2±0.3	1.2±0.3	1.3±0.2	1.5±0.3	1.5±0.3	1.3±0.2*	1.2±0.3	1.2±0.2	1.2±0.2	1.4±0.2	1.3±0.2*

Data are presented as mean±SD. *P<0.05 vs. the corresponding parameter in men.
LV, left ventricle; EDV, end-diastolic volume; ESV, end-systolic volume; BSA, body surface area; EF, ejection fraction; MV ratio, mass to volume ratio.

Table 3. Normal Values of LA Parameters

Age (years)	Men						Women					
	Overall	20–29	30–39	40–49	50–59	60–69	Overall	20–29	30–39	40–49	50–59	60–69
n	222	45	63	43	37	34	139	38	30	27	26	18
Maximum volume, ml	41±11	39±8	40±10	42±12	43±12	43±10	36±9*	34±7*	34±6*	39±9	37±11*	38±10
Minimum volume, ml	17±5	16±4	16±5	18±6	18±6	18±5	15±4*	14±3*	14±3*	16±5	16±6	16±5
Maximum volume/BSA, ml/m²	23±6	22±4	23±5	23±6	24±7	26±6	24±6	23±5	23±5	25±6	25±8	26±6
Minimum volume/BSA, ml/m²	10±3	9±2	9±3	10±3	10±3	11±3	10±3	9±2	9±2	10±3	11±3	11±3
Percent volume change, %	58±6	58±6	60±5	68±5	57±5	57±6	58±6	59±7	59±5	59±6	56±7	60±6

Data are presented as mean±SD. *P<0.05 vs. the corresponding parameter in men.
BSA, body surface area; LA, left atrium.

raphy.[2] Considering the physical and racial differences between Western and Asian populations,[3–5] it is important to establish reference values of echocardiographic parameters for the Japanese population. We have already published details from the Japanese Normal Values for Echocardiographic Measurements Project (JAMP) study to determine the normal values of 2-dimensional echocardiography (2DE).[6,7]

The recently developed real-time 3-dimensional (3D) echocardiography (RT3DE) provides fast and non-invasive 3D estimates with high image resolution that are more accurate and physiologic than those measured by conventional imaging techniques.[8,9] A number of previous studies have revealed the advantages of RT3DE for the assessment of left ventricular (LV) volume, mass and output,[10–12] as well as for the 3D geometry of the heart structure.[13–15] However, the normal values of RT3DE parameters have not been fully investigated, especially for a healthy Japanese population. Therefore, as an extension to the JAMP study with 2DE, this study was designed to determine the normal reference values of RT3DE parameters in a large, healthy Japanese population.

Methods

Study Population

The study population was consisted of 410 healthy volunteers aged from 20 to 69 years (253 males, mean age 42±14 years) at 23 collaborating institutions. None of the subjects had a history of cardiac disease or risk factors. Furthermore, none of the subjects had fever, anemia, or high blood pressure (systolic >135 mmHg or diastolic >85 mmHg) that could have affected the results of echocardiography. All electrocardiographic and 2DE recordings in the recruited subjects were normal. The dataset of RT3DE was obtained from each institution and sent to the Osaka Ekisaikai Hospital for analysis. A single expert

sonographer (T.N.), who had 10 years of experience in echocardiography with approximately 6000 2DE and 200 RT3DE examinations, analyzed the RT3DE dataset. This study was approved by the Ethics Committee of each institution.

Transthoracic 3D Echocardiography

The transthoracic RT3DE was examined by SONOS 7500 and iE-33 (Philips Medical Systems, Andover, MA, USA) in 191 subjects (47%), Vivid 7 and Vivid E9 (GE Medical Systems, Milwaukee, WI, USA) in 150 subjects (37%), SC2000 (Siemens Mountainview, CA, USA) in 41 subjects (10%), and Artida (Toshiba Medical Systems, Tokyo, Japan) in 28 subjects (7%). RT3DE images from the apical view were acquired during a breath hold with electrocardiogram gating. Gain and compression controls as well as the time gain compensation settings were optimized for the quality of the echocardiographic images. All RT3DE data-sets were digitally stored and analyzed off-line.

RT3DE was analyzed using commercially available software for each RT3DE system; QLAB for SONOS 7500 and iE-33, EchoPac (TomTec LV volume) for Vivid 7 and Vivid E9, SC2000 Workplace (eSie LVA) for SC2000, and Advanced Cardiology Package for Artida. The off-line software automatically identified the cavity wall interface in the 3D space throughout the cardiac cycle. Manual adjustments were performed, when necessary, to include the papillary muscles and trabeculae in the LV cavity, and to exclude the left atrial (LA) appendage and pulmonary vein in the LA cavity, respectively. The following parameters were then obtained: (1) LV end-diastolic (EDV), end-systolic volumes (ESV), and ejection fraction (EF); (2) maximal and minimal LA volumes, and percent change; calculated as (diastolic volume−systolic volume)/diastolic volume× 100; and (3) LV mass, and the ratio of LV mass to EDV (MV ratio). LV epicardial borders at the end-diastole were traced for the measurement of LV mass by using the following formula: (end-diastolic epicardial volume−EDV)×1.05. The LV mass was determined by multiplying the volumetric parameter by the specific density of the myocardium (1.05 g/ml).

Each parameter was indexed for body surface area (BSA) when appropriate.

Statistical Analysis

Values were expressed as mean±SD. The parametric data of men and women, and those of multi-beat and single-beat RT3DE systems were compared by using the unpaired t-test. Linear regression was used for the correlation of variables of interest. Differences were considered significant at $P<0.05$. Inter-observer variability for echocardiographic measurements was analyzed in 15 random subjects by 2 independent blinded observers (T.N. and K.M.). Intra-observer variability was analyzed in another group of 15 subjects by the same observer at 2 different time-points. The results were analyzed by using the Bland-Altman method.

Table 4. Relationship Between Age and Various Echocardiographic Parameters

	Men		Women	
	r	P value	r	P value
LV				
EDV	−0.40	<0.001	−0.21	0.01
ESV	−0.37	<0.001	−0.21	0.01
EDV/BSA	−0.36	<0.001	−0.20	0.02
ESV/BSA	−0.34	<0.001	−0.20	0.02
EF	0.08	0.2	0.09	0.3
Mass	−0.13	0.05	0.06	0.5
Mass/BSA	−0.04	0.5	0.11	0.2
MV ratio	0.36	<0.001	0.22	0.009
LA				
Maximum volume	0.14	0.04	0.17	0.04
Minimum volume	0.18	0.009	0.24	0.004
Maximum volume/BSA	0.19	0.004	0.21	0.01
Minimum volume/BSA	0.22	<0.001	0.27	0.001
Percent volume change	−0.12	0.07	−0.16	0.07

Abbreviations see in Tables 2,3.

Results

Feasibility of RT3DE

Among the total of 410 subjects, 54 and 43 subjects were excluded due to inadequate delineation of the chamber wall in images of the LV and LA, respectively. Thus, the feasibility of RT3DE measurement was 87% for LV and 90% for LA.

Values of RT3DE Parameters and Their Relationship to Gender and Age

Table 1 shows the characteristics of 410 healthy subjects by overall, age- and gender-groups. Men were heavier, taller and had larger BSA than women. There were not differences in heart rate between men and women, although blood pressure in men was slightly higher than that in women.

The mean values of LV and LA parameters in overall, age- and gender-groups are shown in Tables 2 and 3, respectively. LV volumes, mass, and LA volumes were larger in men than in women, even after normalization by BSA. There were no significant differences in LVEF and LA percent volume change between men and women. Table 4 summarizes the relationship between age and the RT3DE parameters. LV volumes decreased with age. This relationship was still evident after adjustment for BSA. Age did not correlate with LV mass, and thus the MV ratio increased with age. LA volumes increased with age, whereas its percentage change did not correlate with age. The increases in the maximum and minimum volumes were 0.83 ml/BSA/10 year (y=0.083x+19.7) and 0.46 ml/BSA/10 year (y=0.046x+7.8) for men and 0.87 ml/BSA/10 year (y=0.087x+20.6) and 0.58 ml/BSA/10 year (y=0.058x+7.8) for women, respectively. Table 5 summarized the results of the

Table 5. Intra- and Inter-Observer Variabilities in RT3DE Measurements

	LV				LA		
	EDV	ESV	EF	Mass	Maximum volume	Minimum volume	Percent volume change
Intra-observer variability	2.4 ml	1.2 ml	1.4%	7.9 g	3.3 ml	1.2 ml	3.6%
Inter-observer variability	4.9 ml	4.0 ml	1.7%	8.1 g	2.9 ml	1.7 ml	2.1%

RT3DE, real-time 3-dimensional echocardiography. Other abbreviations see in Tables 2,3.

Bland-Altman analysis.

Discussion

This study evaluated the normal reference values for LV and LA volumes, and their functional parameters, measured on RT3DE in a healthy Japanese population, and analyzed the effects of age and gender on these parameters.

Advantages of RT3DE

In clinical practice, 2DE is generally used as the initial diagnostic imaging modality for evaluation of the structure and function of the cardiovascular system and establishment of clinical diagnosis. However, it is clear that geometric assumption in quantification of chamber volume precludes a precise measurement using 2DE. Recently, 3D imaging techniques, including RT3DE, magnetic resonance imaging (MRI) and computed tomography (CT), have provided unique anatomic views of different cardiac structures as well as accurate quantification of LV volume, mass and output. However, the utility of cardiac MRI and CT might be restricted, especially in sequential or follow-up studies, by their inherent limitations, such as expense, being time-consuming, the use of a contrast agent, and radiation exposure (CT only). The developed RT3DE offers an opportunity for rapid, non-invasive, physiologic image acquisition with high image quality and good reproducibility, which would be more feasible than other 3D imaging techniques.[16] However, the lack of the reference values might have so far, at least in part, limited the use of RT3DE in the clinical and research mainstream in the field of cardiovascular disease.

Comparison With Previous 2DE Observations

In a comparison with our previous 2DE observations,[6] LV and LA volumes were similar between RT3DE and 2DE. For example, LV EDV/BSA of RT3DE and 2DE was 50±12 ml/m^2 and 53±11 ml/m^2 for men and 46±9 ml/m^2 and 49±11 ml/m^2 for women, respectively. It is recognized that volume quantification of 2DE using the biplane Simpson disk method has limitations of image plane positioning errors and geometric assumptions, which results in low reproducibility and tendency to underestimate absolute volume, especially in the remodeling heart.[2] However, our results indicated that in the experienced laboratories that are aware of the above-mentioned limitations of 2DE, volumetric quantification using the biplane Simpson disk method is acceptable at least for normal-shaped hearts, and the same normal reference values of LV and LA volumes can be used between RT3DE and 2DE.

In contrast, LV mass/BSA of RT3DE (64±12 g/m^2 for men and 56±11 g/m^2 for women) tended to be smaller than those of 2DE based on the area-length formula (76±16 g/m^2 for men and 70±14 g/m^2 for women). This observation was supported by a previous study that showed that LV mass was underestimated by RT3DE and overestimated by 2DE, as compared with MRI findings.[8] Furthermore, low reproducibility of 2DE for LV mass measurement has been reported.[8,17,18] Therefore, the difference in the normal reference value between RT3DE and 2DE should be taken into the consideration when determining the presence or absence of LV hypertrophy in clinical practice.

Relationship to Age, Gender and Race

It is generally accepted that age-related changes in cardiac structure and function occur in healthy subjects. Our results of age-related changes of the heart are consistent with the findings of previous studies in normal subjects using 2DE,[6] MRI,[19–21] and CT.[22] LV size decreases with age, whereas LV mass remains unchanged. This LV remodeling indicates age-related LV "concentric hypertrophy" as a response to increased arterial pressure and afterload with age. LV volume declines are likely offset by elevated or maintained LVEF. In contrast, LA volumes slightly increase with age, which might reflect age-related LV diastolic dysfunction.[23,24] Such LA remodeling due to age-related LV diastolic dysfunction might be subtle enough to be determined by 2DE. In fact, our previous 2DE study found a discrepancy in the result, that LA length in antero-posterior direction increased with age, although the estimated LA volume, calculated from 2 orthogonal 2D planes, was unchanged.[6]

In the present study, LV size was larger in men than in women. This gender difference became smaller after correction for BSA, which is similar to the results of previous reports.[19,25]

Two studies have previously examined the reference values of RT3DE parameters in healthy subjects. In the study by Aune et al from Norway, the mean value of EDV was 136 ml in men and 104 ml in women.[26] Even after correction for BSA (2.05 m^2 for men and 1.78 m^2 for women), these values are still lager than our results (66 ml/m^2 vs. 50 ml/m^2 in men, and 5 ml/m^2 vs. 46 ml/m^2, respectively). A previous JAMP study of 2DE confirmed that Japanese hearts were smaller than those of the Western population.[6] These observations strongly indicate the existence of race-related differences in echocardiographic measurements. Kaku et al recently investigated the growing process of LV geometry in 280 healthy subjects, between the age of 1 to 88 years.[27] These subjects were enrolled in Japan and the USA. Because of the race differences in the heart,[3–6,26] the use of their results as the Japanese reference values might be limited. Our study is the first that provides age- and gender-specific reference values of RT3DE parameters in a large, healthy Japanese population. These results should be helpful for disease classification, stratification of risk, and guidance of therapy using RT3DE.

Study Limitations

This study has several limitations. Although all subjects were interviewed by physicians in participating institutions, one cannot rule out the presence of an unrecognized cardiovascular disease. Furthermore, the differences among the RT3DE systems might affect the results of this study. Although no significant differences were observed in RT3DE results between multi-beat and single-beat RT3DE systems among all 10 age- and gender-subgroups (multi-beat: SONOS 7500, iE-33, Vivid 7, and Artida; single-beat: Vivid E9 and SC2000), the impact of the differences among 7 different echo systems on the results remained unknown because of a relatively small number of subjects in each age- and gender-subgroup ranged approximately from 20 to 60. The number of examinations with Artida (n=28), Vivid E9 (n=15) and SC2000 (n=41), which were introduced within several recent years, were low. Therefore, future investigations might be necessary to answer this question. Also, RT3DE was performed at each institution, and analysis was completed by experienced sonographers in the center, who were blinded to clinical information. These processes might be different to real, clinical situations, which might influence the reproducibility of RT3DE results. Finally, although there were significant correlations between age and LA volumes, these age-related changes in LA volume were relatively small, and therefore, further investigations are necessary to evaluate the importance of age-related LA volume

changes in clinical practice.

Conclusions

Our multicenter investigation provided normal reference values for LV and LA volumes, and their functional correlates from RT3DE in a large, healthy Japanese population. The results of analysis showed age- and gender-differences in these parameters. The results of present study should be considered in the clinical and research studies that use RT3DE for the management of cardiovascular disease.

Acknowledgments

This work was supported, in part, by a research grant from the Fukuda Foundation for Medical Technology, Japan.

Disclosures

The authors declare no conflict of interest.

References

1. Okura H, Takada Y, Yamabe A, Ozaki T, Yamagishi H, Toda I, et al. Prevalence and correlates of physiological valvular regurgitation in healthy subjects. *Circ J* 2011; **75:** 2699–2704.
2. Lang RM, Bierig M, Devereux RB, Flachskampf FA, Foster E, Pellikka PA, et al. Recommendations for chamber quantification: A report from the American Society of Echocardiography's Guidelines and Standards Committee and the Chamber Quantification Writing Group, developed in conjunction with the European Association of Echocardiography, a branch of the European Society of Cardiology. *J Am Soc Echocardiogr* 2005; **18:** 1440–1463.
3. Hinderliter AL, Light KC, Willis PW 4th. Racial differences in left ventricular structure in healthy young adults. *Am J Cardiol* 1992; **69:** 1196–1199.
4. Harshfield GA, Koelsch DW, Pulliam DA, Alpert BS, Richey PA, Becker JA. Racial differences in the age-related increase in left ventricular mass in youths. *Hypertension* 1994; **24:** 747–751.
5. Schieken RM, Schwartz PF, Goble MM. Tracking of left ventricular mass in children: Race and sex comparisons: The MCV Twin Study: Medical College of Virginia. *Circulation* 1998; **97:** 1901–1906.
6. Daimon M, Watanabe H, Abe Y, Hirata K, Hozumi T, Ishii K, et al. Normal values of echocardiographic parameters in relation to age in a healthy Japanese population: The JAMP study. *Circ J* 2008; **72:** 1859–1866.
7. Daimon M, Watanabe H, Abe Y, Hirata K, Hozumi T, Ishii K, et al. Gender differences in age-related changes in left and right ventricular geometries and functions. *Circ J* 2011; **75:** 2840–2846.
8. Jenkins C, Bricknell K, Hanekom L, Marwick TH. Reproducibility and accuracy of echocardiographic measurements of left ventricular parameters using real-time three-dimensional echocardiography. *J Am Coll Cardiol* 2004; **44:** 878–886.
9. Shiota T. Clinical application of 3-dimensional echocardiography. *J Echocardiogr* 2005; **3:** 93–103.
10. Mor-Avi V, Sugeng L, Weinert L, MacEneaney P, Caiani EG, Koch R, et al. Fast measurement of left ventricular mass with real-time three-dimensional echocardiography: Comparison with magnetic resonance imaging. *Circulation* 2004; **110:** 1814–1818.
11. Pemberton J, Li X, Karamlou T, Sandquist CA, Thiele K, Shen I, et al. The use of live three-dimensional Doppler echocardiography in the measurement of cardiac output: An in vivo animal study. *J Am Coll Cardiol* 2005; **45:** 433–438.
12. Takeuchi M, Nishikage T, Mor-Avi V, Sugeng L, Weinert L, Nakai H, et al. Measurement of left ventricular mass by real-time three-dimensional echocardiography: Validation against magnetic resonance and comparison with two-dimensional and M-mode measurements. *J Am Soc Echocardiogr* 2008; **21:** 1001–1005.
13. Watanabe N, Ogasawara Y, Yamaura Y, Kawamoto T, Toyota E, Akasaka T, et al. Quantitation of mitral valve tenting in ischemic mitral regurgitation by transthoracic real-time three-dimensional echocardiography. *J Am Coll Cardiol* 2005; **45:** 763–769.
14. Daimon M, Shiota T, Gillinov AM, Hayase M, Ruel M, Cohn WE, et al. Percutaneous mitral valve repair for chronic ischemic mitral regurgitation: A real-time three-dimensional echocardiographic study in an ovine model. *Circulation* 2005; **111:** 2183–2189.
15. Fukuda S, Saracino G, Matsumura Y, Daimon M, Tran H, Greenberg NL, et al. Three-dimensional geometry of the tricuspid annulus in healthy subjects and in patients with functional tricuspid regurgitation: A real-time, 3-dimensional echocardiographic study. *Circulation* 2006; **114:** I492–I498.
16. Hare JL, Jenkins C, Nakatani S, Ogawa A, Yu CM, Marwick TH. Feasibility and clinical decision-making with 3D echocardiography in routine practice. *Heart* 2008; **94:** 440–445.
17. Qin JX, Jones M, Travaglini A, Song JM, Li J, White RD, et al. The accuracy of left ventricular mass determined by real-time three-dimensional echocardiography in chronic animal and clinical studies: A comparison with postmortem examination and magnetic resonance imaging. *J Am Soc Echocardiogr* 2005; **18:** 1037–1043.
18. Oe H, Hozumi T, Arai K, Matsumura Y, Negishi K, Sugioka K, et al. Comparison of accurate measurement of left ventricular mass in patients with hypertrophied hearts by real-time three-dimensional echocardiography versus magnetic resonance imaging. *Am J Cardiol* 2005; **95:** 1263–1267.
19. Sandstede J, Lipke C, Beer M, Hofmann S, Pabst T, Kenn W, et al. Age- and gender-specific differences in left and right ventricular cardiac function and mass determined by cine magnetic resonance imaging. *Eur Radiol* 2000; **10:** 438–442.
20. Nikitin NP, Loh PH, de Silva R, Witte KK, Lukaschuk EI, Parker A, et al. Left ventricular morphology, global and longitudinal function in normal older individuals: A cardiac magnetic resonance study. *Int J Cardiol* 2006; **108:** 76–83.
21. Cheng S, Fernandes VR, Bluemke DA, McClelland RL, Kronmal RA, Lima JA. Age-related left ventricular remodeling and associated risk for cardiovascular outcomes: The Multi-Ethnic Study of Atherosclerosis. *Circ Cardiovasc Imaging* 2009; **2:** 191–198.
22. Lin FY, Devereux RB, Roman MJ, Meng J, Jow VM, Jacobs A, et al. Cardiac chamber volumes, function, and mass as determined by 64-multidetector row computed tomography: Mean values among healthy adults free of hypertension and obesity. *JACC Cardiovasc Imaging* 2008; **1:** 782–786.
23. Sohn DW, Chai IH, Lee DJ, Kim HC, Kim HS, Oh BH, et al. Assessment of mitral annulus velocity by Doppler tissue imaging in the evaluation of left ventricular diastolic function. *J Am Coll Cardiol* 1997; **30:** 474–480.
24. Abhayaratna WP, Seward JB, Appleton CP, Douglas PS, Oh JK, Tajik AJ, et al. Left atrial size: Physiologic determinants and clinical applications. *J Am Coll Cardiol* 2006; **47:** 2357–2363.
25. Byrd BF 3rd, Wahr D, Wang YS, Bouchard A, Schiller NB. Left ventricular mass and volume/mass ratio determined by two-dimensional echocardiography in normal adults. *J Am Coll Cardiol* 1985; **6:** 1021–1025.
26. Aune E, Baekkevar M, Rodevand O, Otterstad JE. Reference values for left ventricular volumes with real-time 3-dimensional echocardiography. *Scand Cardiovasc J* 2010; **44:** 24–30.
27. Kaku K, Takeuchi M, Otani K, Sugeng L, Nakai H, Haruki N, et al. Age- and gender-dependency of left ventricular geometry assessed with real-time three-dimensional transthoracic echocardiography. *J Am Soc Echocardiogr* 2011; **24:** 541–547.

Appendix

We appreciate the assistance of many colleagues in the echocardiographic recordings and management: Kumiko Maeda, RMS, Reiko Miyahana, RMS (Osaka Ekisaikai Hospital); Kiyomi Saito, RMS (Sakakibara Heart Institute); Sakiko Miyazaki, MD, Yoko Koiso, MD (Juntendo University School of Medicine); Noriyo Fujii, RMS, Rieko Nakamura, RMS (Osaka City General Hospital); Hiroki Matsubara, RMS, Kaori Kato, RMS (Nagoya University Hospital); Yuko Wakinishi, RMS, Nozomi Wada, MD (Wakayama Medical University); Hiroki Oe, MD (Okayama University Graduate School of Medicine); Shuichi Takahashi, JRDCS (Tenri Hospital); Hiroto Utsunomiya, MD, Yasuki Kihara, MD (Hiroshima University Hospital); Akira Kisanuki, MD, Kunitsugu Takasaki, MD (Kagoshima University); Yasuaki Wada, MD, Kosuke Uchida, MD (Yamaguchi University Hospital); Rieko Takahashi, MD (Gunma University Graduate School of Medicine); Tomoko Takada, RMS (Gunma University Hospital); Ayako Tomita, RMS (Saiseikai Kumamoto Hospital), Shinichi Iwata, MD, Nobuhiro Nonaka, RMS (Fuchu Hospital); Hiroyuki Okura, MD, Kiyoshi Yoshida, MD (Kawasaki Medical School); Hideaki Yoshino, MD, Kazuki Satou, MD (Kyorin University School of Medicine); Yasuyoshi Takei, MD, Nori Takahashi, RMS (Tokyo Medical University); Hiroyuki Iwano, MD (Hokkaido University Graduate School of Medicine); Sanae Kaga, RMS (Hokkaido University Hospital); Yasushi Sakata, MD, Yasuharu Takeda, MD (Osaka University Graduate School of Medicine).

Usefulness of the Right Parasternal Approach to Evaluate the Morphology of Atrial Septal Defect for Transcatheter Closure Using Two-Dimensional and Three-Dimensional Transthoracic Echocardiography

Nobuhisa Watanabe, RDCS, Manabu Taniguchi, MD, Teiji Akagi, MD, Yasuharu Tanabe, RDCS, Norihisa Toh, MD, Kengo Kusano, MD, Hiroshi Ito, MD, Norio Koide, MD, and Shunji Sano, MD, *Okayama, Japan*

Background: The aim of this study was to demonstrate the feasibility and usefulness of addition of the right parasternal approach to the conventional left parasternal and apical approaches using two-dimensional (2D) and three-dimensional (3D) transthoracic echocardiography (TTE) for morphologic evaluation in cases of transcatheter closure of atrial septal defects (ASDs).

Methods: In 112 consecutive patients with ASDs, the morphology of the defects was evaluated for transcatheter closure in the right parasternal view in addition to the conventional left views using 2D and 3D TTE. Measurements of the maximal ASD diameter and detection of deficient rim obtained on 2D TTE were compared with those obtained by 2D transesophageal echocardiography. The shapes and locations of ASDs visualized by 3D TTE were compared with those visualized by 3D transesophageal echocardiography.

Results: In 88 patients (80.0%), optimal images from the right parasternal approach for morphologic evaluation of ASDs were obtained. Although there was a significant difference in maximal ASD diameter obtained only in the conventional left approach compared with transesophageal echocardiographic measurements ($P < .05$), when the right parasternal approach was applied, a significant difference was not found ($P = .18$), and the diagnostic concordance of the rim deficiency was improved from 85.2% to 90.9%. Three-dimensional TTE from the right parasternal approach improved visualization of the shape and location of ASDs from 65.5% to 74.5%.

Conclusions: Additional use of the right parasternal approach enables detailed morphologic evaluation for transcatheter closure of ASDs. In patients with suboptimal images on 3D TTE in the left conventional approach, additional 3D TTE in the right parasternal approach can improve the feasibility of obtaining optimal 3D images to evaluate the shapes and locations of ASDs. (J Am Soc Echocardiogr 2012;25:376-82.)

Keywords: Right parasternal approach, Transthoracic echocardiography, Transesophageal echocardiography, Atrial septal defect

Transcatheter closure of atrial septal defects (ASDs) has recently become established as a safe and effective treatment, and the procedure has become an alternative to a surgical approach.[1-5] Appropriate patient selection for transcatheter closure is the most important factor for success in this procedure,[4] and morphologic evaluation, including evaluation of maximal ASD diameter and surrounding rims by echocardiography, is essential. Although two-dimensional (2D) transthoracic echocardiography (TTE) in the left parasternal, apical, and subcostal views is routinely used for this purpose, previous studies have demonstrated that these views enable only limited morphologic evaluation of ASDs.[6-9] Real-time three-dimensional (3D) echocardiography, in which a comprehensible en face view of ASDs is obtained, has been available in a clinical setting.[10-12] Three-dimensional TTE is expected to improve understanding of the morphology of ASDs, but data are limited, and it is difficult to obtain good-quality images on 3D TTE using the left parasternal and apical approaches.[13-15] In this regard, 2D transesophageal echocardiography (TEE) and 3D TEE have been widely accepted and established as diagnostic modalities in evaluation of the morphology of ASDs for transcatheter closure because of their high-quality imaging[16-21]; however, TEE has a semi-invasive nature.

The right parasternal approach, in which the transducer is placed to the right of the sternum in the right lateral decubitus position, was

From the Division of Medical Support (N.W., Y.T.) and the Division of Cardiac Intensive Care Unit (M.T., T.A.), Okayama University Hospital, Okayama, Japan; the Department of Cardiovascular Medicine (N.T., K.K., H.I.), the Department of Laboratory Medicine (N.K.), and the Department of Cardiovascular Surgery (S.S.), Okayama University Graduate School of Medicine, Dentistry and Pharmaceutical Sciences, Okayama, Japan.

Reprint requests: Manabu Taniguchi, MD, 2-5-1 Kita-ku Shikata-Cho, Okayama 700-8558, Japan (E-mail: *tmnb@md.okayama-u.ac.jp*).

0894-7317/$36.00

Copyright 2012 by the American Society of Echocardiography.

doi:10.1016/j.echo.2012.01.002

Abbreviations

ASD = Atrial septal defect

TEE = Transesophageal echocardiography

3D = Three-dimensional

TTE = Transthoracic echocardiography

2D = Two-dimensional

reported to enable better visualization of ASDs and evaluation of the direction of shunt flow in patients with ASDs because it obtains a longitudinal vena cava superior-inferior plane of the interatrial septum.[22-26] In addition, 3D TTE in this approach might improve the feasibility of obtaining optimal en face images of ASDs. However, there have been limited data on the usefulness of the right parasternal approach using 2D and 3D TTE for morphologic evaluation in cases of transcatheter closure. Therefore, we sought to assess the usefulness of the right parasternal approach in addition to the conventional left parasternal and apical approaches in evaluating ASD morphology for the suitability of transcatheter closure using 2D and 3D TTE.

METHODS

Study Population

A total of 112 consecutive patients (40 men and 72 women) were prospectively evaluated for transcatheter closure of ASDs using the Amplatzer Septal Occluder (AGA Medical Corporation, Plymouth, MN) with 2D and 3D TTE. Two patients with ASDs other than the secundum type were excluded from this study (one had a superior sinus venosus ASD and the other had an unroofed coronary sinus ASD). Therefore, 110 patients were included in the study. All patients except for one were referred from other hospitals to our institution for transcatheter ASD closure. Age at the examination ranged from 6 to 84 years (mean, 46.1 ± 20.5 years). Two-dimensional TEE and 3D TEE were performed <3 days after TTE by a blinded observer. The study was approved by the local ethics committee.

Two-Dimensional TTE

Two-dimensional TTE was performed using a commercially available ultrasound system with a 3.5-MHz transducer (Vivid 7; GE Healthcare, Wauwatosa, WI). Right ventricular midcavity diameter was measured in the apical four-chamber view according to the guideline of American Society of Echocardiography.[27] In all patients, the morphology of ASDs was evaluated using TTE in the left lateral decubitus position from the left parasternal and apical approaches (conventional left approach). Then a transducer was positioned on the right parasternal border with the patient in the right lateral decubitus position (right parasternal approach). Maximal ASD diameter and the minimal diameter of surrounding rims were measured at end-systole by carefully sweeping the transducer from right to left and top to bottom of the interatrial septum in both approaches. Regarding the maximal ASD diameter, first, the ASD diameter was measured using the conventional left approach (ASD_L diameter), and then the ASD diameter was measured by the right parasternal approach (ASD_R diameter). The maximal ASD diameter was considered the maximal value from measurements by both approaches. The surrounding rims were classified according to location as superoanterior, inferoanterior, superoposterior, or inferoposterior. The superoanterior rim was measured as the distance between the aorta and the defect. The inferoanterior rim was measured as the distance from the atrioventricular valves. The inferoposterior rim was measured as the distance from the left atrial wall. The superoposterior rim was measured as the distance from the defect to the superior vena cava and to determine the inferoposterior rim as the distance from the defect to the inferior vena cava (Figure 1). Any rim length < 5 mm was considered deficient. First, the presence or absence of a deficient rim was evaluated using the conventional left approach, and then the right parasternal approach was used.

Three-Dimensional TTE

Three-dimensional TTE was performed after 2D TTE using a commercially available ultrasound system with a 3V transducer (Vivid 7). In all patients, the left parasternal approach was first chosen and optimized, and then loops from five consecutive cycles were acquired and digitally stored. In cases with suboptimal 3D images by the left parasternal approach, we attempted to obtain optimal 3D images using the right parasternal approach. In all patients, at least three acquisitions were performed, and the data set with the best image quality was chosen for analysis. The shapes and locations of ASDs were visually evaluated on the best 3D images.

Two-Dimensional and 3D TEE

Two-dimensional and 3D TEE were performed using a commercially available ultrasound system (iE33; Philips Medical Systems, Andover, MA). Maximal ASD diameter (ASD_{TEE} diameter) and minimal diameter of the surrounding rims were assessed at end-systole using both 2D TEE and 3D TEE, as previously reported.[18] To evaluate surrounding rims using 2D TEE, the superoanterior rim was measured as the distance between the aortic annulus and the defect in the horizontal plane at 0° to 30°. The inferoanterior rim was measured as the distance between the defect and atrioventricular valves in the four-chamber view at 135°. The longitudinal plane around 90° was used to determine the superoposterior rim as the distance from the defect to the superior vena cava and to determine the inferoposterior rim as the distance from the defect to the inferior vena cava (Figure 1). The rim length was considered deficient if the length was <5 mm.

Real-time 3D transesophageal echocardiographic data were obtained after a complete 2D transesophageal echocardiographic study. Real-time 3D zoom mode, which displays a smaller, magnified pyramidal data set, was used to evaluate the shapes and locations of ASDs as well as the rough relation to surrounding structures.

Two-dimensional and 3D transesophageal echocardiographic data were considered reference standards. In patients with optimal images obtained on both approaches, ASD_{TEE} diameter and detection of deficient rims obtained on 2D TEE were compared with those obtained on 2D TTE. The shapes and locations of ASDs using 3D TTE were compared with those obtained using 2D and 3D TEE.

Measurement Variability

ASD diameter and the minimal diameter of the surrounding rims obtained using TTE were measured by two independent observers and by one observer two times 1 month apart in 10 randomly selected patients to determine interobserver variability and intraobserver variability. Variability was assessed as the absolute difference between two measurements expressed as a percentage of their mean values.

Statistical Analysis

Categorical data are expressed as numbers and percentages and continuous data as mean ± SD. The significance of baseline differences

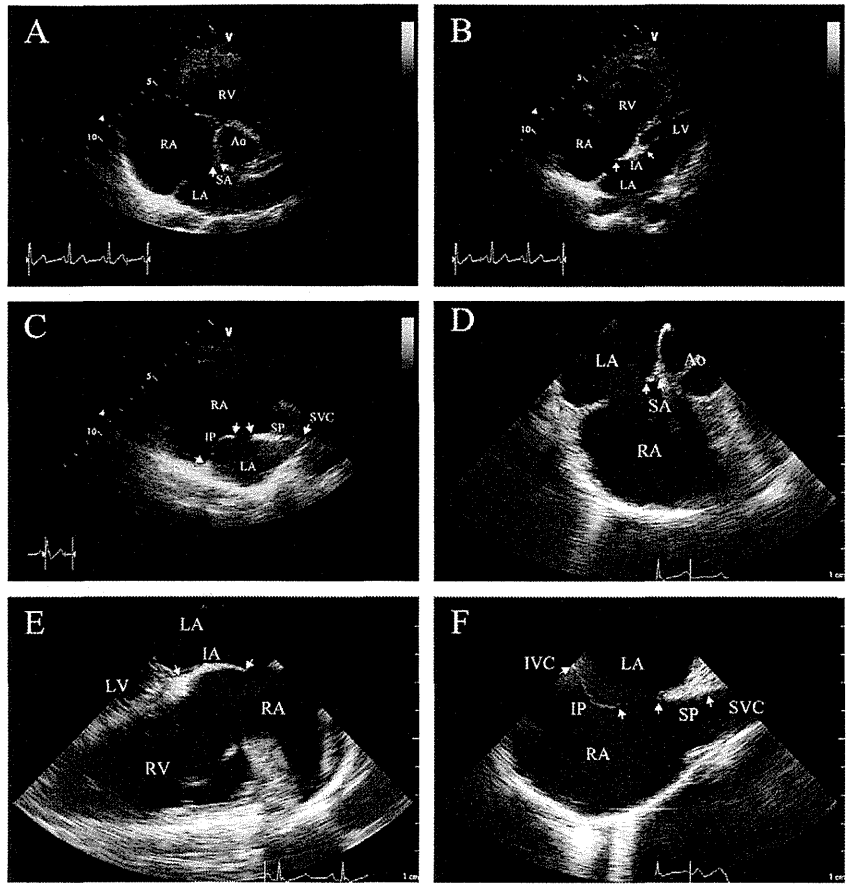

Figure 1 Measurement of maximal ASD diameter and the surrounding rims on 2D TTE and 2D TEE. The surrounding rim is measured from mark (*white arrow*) to mark (*white arrow*). **(A)** Left parasternal short-axis view, **(B)** left parasternal four-chamber view, **(C)** right parasternal longitudinal view, **(D)** short-axis transesophageal echocardiographic view (0°–30°), **(E)** four-chamber transesophageal echocardiographic view (135°), **(F)** biatrial transesophageal echocardiographic view (90°). The surrounding rims are measured at end-systole (*white arrow*). *Ao*, Aorta; *IA*, inferoanterior rim; *IP*, inferoposterior rim; *IVC*, inferior vena cava; *LA*, left atrium; *LV*, left ventricle; *RA*, right atrium; *RV*, right ventricle; *SA*, superoanterior rim; *SP*, superoposterior rim; *SVC*, superior vena cava.

was determined using paired and unpaired t tests as appropriate. Categorical variables are expressed as counts and percentages and were compared using χ^2 or Fisher's exact tests as appropriate. Comparisons between measurements were done using Pearson's linear regressions analysis. The agreement of the two methods was evaluated using the Bland-Altman test. P values $< .05$ were considered statistically significant. Statistical analyses were done using SPSS version 18.0 (SPSS, Inc., Chicago, IL).

RESULTS

Baseline Characteristics of Study Population

Table 1 shows the baseline characteristics and 2D transthoracic echocardiographic parameters of the study population. All patients showed hemodynamically significant atrial shunts or the presence of right atrial and ventricular volume overload.

Feasibility of 2D TTE in the Right Parasternal Approach

Two-dimensional TTE with the conventional left approach enabled the detection of shunt flow on color-flow Doppler imaging and visualization of the optimal images for the measurement of defects in all patients. Detection of shunt flow in the right parasternal approach on color-flow Doppler images was successful in 102 patients (92.7%). Optimal images with the right parasternal approach for measurements of defects and surrounding rims were visualized in 88 patients (80.0%). When all patients were divided into two groups according to age, <40 years ($n = 42$; mean age, 24.1 ± 10.4 years) and ≥40 years ($n = 68$; mean age, 59.6 ± 11.5 years), the percentage of patients in whom optimal images to measure ASD diameter and surrounding

Table 1 Baseline characteristics and transthoracic echocardiographic parameters of the study population ($n = 110$)

Variable	Value
Men/women	39/71
Age (y)	46.1 ± 20.5 (6–84)
Height (m)	1.58 ± 0.12 (1.13–1.83)
Weight (kg)	54 ± 12.3 (17–92)
Body surface area (m^2)	1.53 ± 0.22 (0.75–2.14)
Right ventricular midcavity diameter (mm)	41.8 ± 5.4 (28–55)
Pulmonary flow/systemic flow ratio	2.4 ± 0.7 (1.2–4.1)

Data are expressed as numbers or as mean ± SD (range).

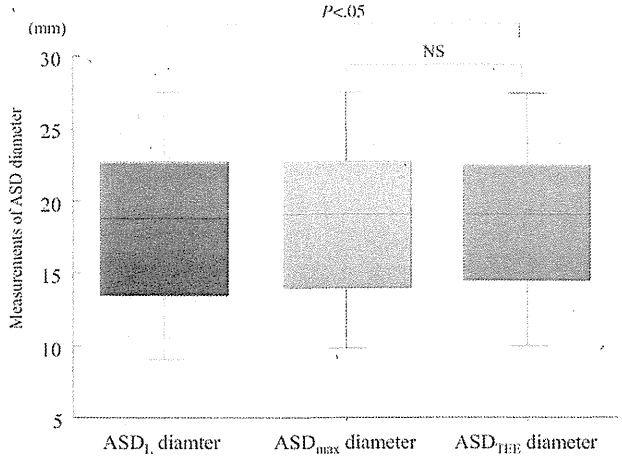

Figure 2 Box plots showing the comparison ASD_L diameter obtained with the conventional left approach (*red box*), maximal ASD diameter obtained with both the left conventional and right parasternal approaches (*orange box*), and ASD_{TEE} diameter (*blue box*).

rim were obtained in the right parasternal approach was significantly higher in those aged <40 years than in those aged ≥40 years (90.5% vs 73.5%, $P = .033$).

Data for the 88 patients in whom optimal 2D transthoracic echocardiographic images for measurements of ASD diameter and surrounding rims were obtained by both approaches were analyzed in our study.

Morphologic Evaluation with 2D TTE and TEE

Maximal ASD diameters between ASD_L diameter, maximal ASD diameter, and ASD_{TEE} diameter were compared in 88 patients with optimal images from the right parasternal approach. There was a small but significant difference between ASD_L diameter and ASD_{TEE} diameter (18.5 ± 6.9 vs 19.0 ± 6.9 mm, $P < .05$). However, when the diameter obtained with the right parasternal approach was taken into account in addition to the diameter obtained with the conventional left approach, a significant difference was not found between measurements of maximal ASD diameter and ASD_{TEE} diameter (18.8 ± 6.7 mm, $P = .18$; Figure 2). Bland-Altman analysis showed the smallest mean absolute differences and narrower limits of agreement when the measurement from the right parasternal approach was added to that from the conventional left approach (Figure 3).

TEE demonstrated that 17 patients (19.3%) had centrally positioned ASD, 55 (62.5%) had superoanterior rim deficiencies, three (3.4%) had inferoposterior deficiencies, five (5.7%) had both superoanterior and inferoposterior deficiencies, and eight (9.1%) had multiple ASDs. Although the detection of a deficient rim showed concordance in 75 patients (85.2%) between TTE with the conventional left approach and 2D TEE, diagnostic concordance was improved to 90.9% by adding the right parasternal approach. In nine patients with inferoposterior rim deficiencies, diagnostic accuracy of the rim deficiency was improved from 66.7% to 100% when the right parasternal approach was added to the conventional left approach.

Evaluation of ASDs with 3D TTE

Although 3D TTE from the left parasternal approach could visualize the 3D optimal image for understanding the shape and location of

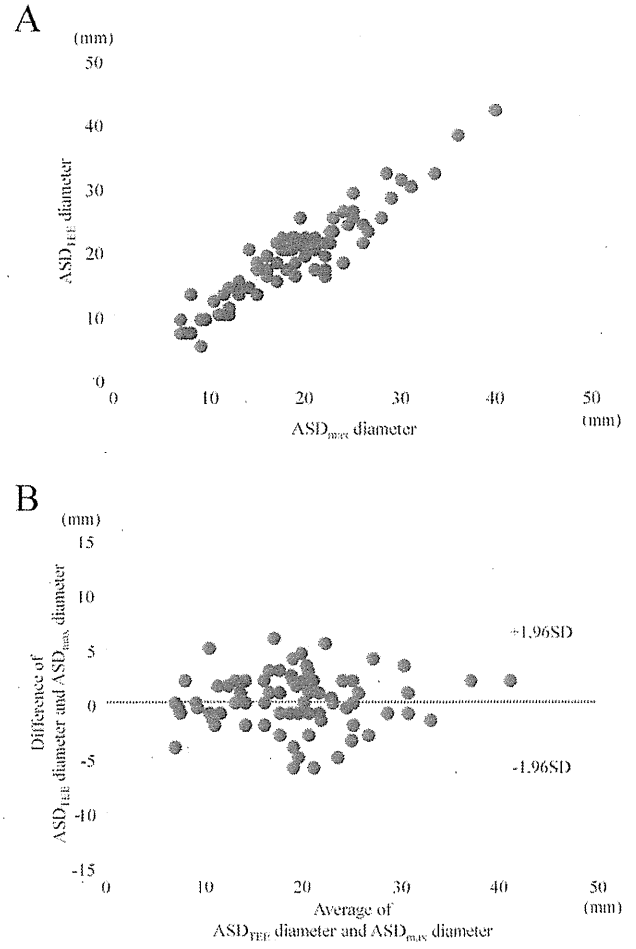

Figure 3 **(A)** Correlations of maximal ASD diameter measured by 2D TTE versus 2D TEE. **(B)** Bland-Altman plot of ASD diameter difference between the measurements on 2D TTE and those on 2D TEE as a function of the average measurements. The *thick continuous line* and *dotted line* indicate the mean ± 1.96 SD of the difference, respectively.

ASDs in only 72 patients (65.5%), the use of the right parasternal approach improved the visualization of optimal 3D TTE images to 74.5% (Figures 4 and 5).

Measurement Variability

Interobserver and intraobserver variability were 1.1% and 0.6%, respectively, for ASD diameter measured by 2D TTE; 6.1% and 6.8%, respectively, for superoposterior rim measurement by 2D TTE; and 9.7% and 8.0%, respectively, for inferoposterior rim measurement by 2D TTE.

DISCUSSION

Our study demonstrated that 2D TTE with the addition of the right parasternal approach to the conventional left approach is feasible and enables evaluation of the morphology of ASDs for transcatheter closure with satisfactory accuracy compared with evaluation by 2D TEE. In particular, the right parasternal approach contributes greatly

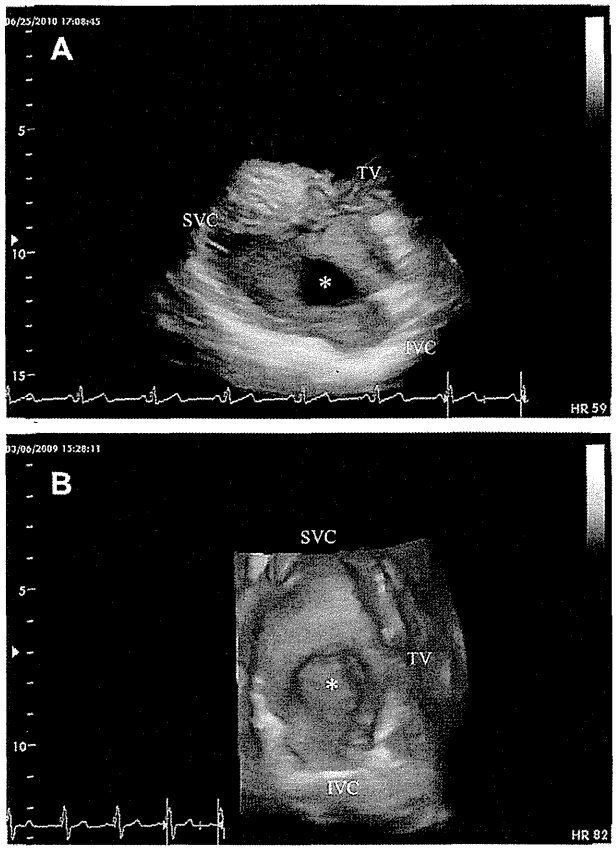

Figure 4 Three-dimensional transthoracic echocardiography of various shapes of the secundum-type ASD (*asterisk*) viewed from the right atrium. **(A)** Superoanterior rim deficient from the left parasternal approach, **(B)** inferoposterior rim deficient from the right parasternal approach. *IVC*, Inferior vena cava; *SVC*, superior vena cava; *TV*, tricuspid valve.

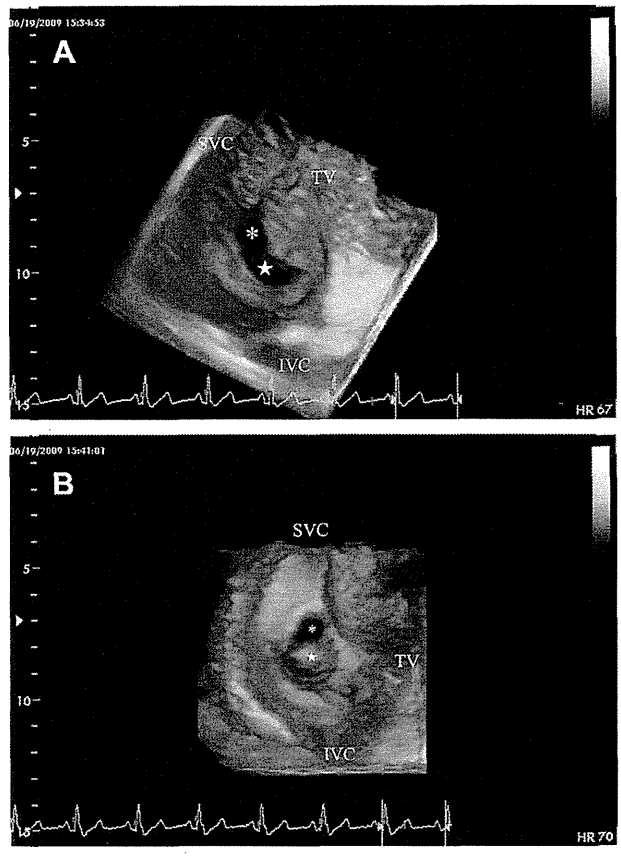

Figure 5 Three-dimensional TTE of the secundum-type ASD (*asterisk*) with an atrial septal aneurysmal (ASA) viewed from the right atrium. **(A)** The ASA (*white star*) was dropped out from the left parasternal approach **(B)** but was clearly visualized from the right parasternal approach. *IVC*, Inferior vena cava; *SVC*, superior vena cava; *TV*, tricuspid valve.

to the identification of rim deficiency, especially in patients with inferoposterior rim deficiencies. In terms of the acquisition of optimal 3D transthoracic echocardiographic images, the addition of the right parasternal approach to the conventional left approach can improve the feasibility of ASD morphologic evaluation.

Feasibility of the Right Parasternal Approach

Previous studies have shown that the right parasternal approach is a reliable technique for detection of ASDs.[22-26] Iliceto *et al.*[25] reported that ASDs were identified using the right parasternal approach in 13 of 17 patients (76.5%) and that the right parasternal approach improved the feasibility of 2D TTE for the detection of ASDs. In our study, we could detect ASDs on color-flow Doppler imaging by 2D TTE using the right parasternal approach with high sensitivity (92.7%). Advances in the technology of echocardiography may have greatly contributed to its high feasibility compared with previous studies. In our study, optimal images in the right parasternal approach were obtained more frequently in younger patients than in older patients, who sometimes have obesity or lung disease. A previous study also demonstrated that the right parasternal view was often easily obtainable in neonates and young children.[26] Therefore, especially in younger patients with intolerance of TEE, TTE including the right parasternal approach can contribute to evaluating ASD morphology for transcatheter closure.

Morphologic Evaluation of ASDs

Previous studies have demonstrated that appropriate patient selection is essential for successful transcatheter closure of ASDs using the Amplatzer Septal Occluder.[16,17] Two crucial parameters, maximal ASD diameter to choose an appropriately sized device and tissue rim dimensions all around the defect to optimize placement of the device, should be measured to select patients for transcatheter closure of ASDs in addition to detection of atrial shunts or echocardiographic findings of right ventricular volume overload.[12] Although TEE is considered the gold standard in evaluating ASD morphology for the suitability of transcatheter closure, TEE has a semi-invasive nature. TTE used to perform a detailed morphologic evaluation of ASDs before TEE can lead to avoiding oversight and shortening transesophageal examination time. Therefore, detailed morphologic evaluation, including evaluation of maximal ASD diameter and surrounding rims by TTE, is important. In our study, the use of the additional right parasternal approach in TTE improved measurements of maximal ASD diameter and detection of rim deficiencies and enabled morphologic evaluation comparable with that obtained by TEE. In the conventional left approach, because the

direction of the ultrasound beam is almost parallel to the interatrial septum, there is frequent dropout of interatrial septal echoes in the region of the mid portion (fossa ovalis). Previous studies have shown that echo dropout in the region of the mid portion frequently occurs and can lead to false diagnoses of large defects.[22,28,29] One of those previous studies showed that the maximal ASD diameter measured with 2D TTE was larger than that measured with 2D TEE and that there was a poor correlation between these measurements because of dropout in the region of the fossa ovalis.[29] The subcostal approach is another useful method for visualizing perpendicularly the interatrial septum.[28] Although 2D TTE from the subcostal approach enables the detection of shunt flow across ASDs easily in pediatric patients,[25,28] this approach can provide suboptimal images or incomplete clinical information with regard to morphologic evaluation for transcatheter ASDs closure, especially in adult patients, because of the limited echocardiographic window.[6-8] The right parasternal approach is a method that can provide better evaluation of the structure of the interatrial septal because the ultrasound beam passes in a plane perpendicular to the interatrial septal.[22-26] The use of the right parasternal approach provided better visualization of the superior vena cava and inferior vena cava entering into the right atrium. The right parasternal approach contributed greatly to the detection of deficient rims in the present study, particularly for the inferoposterior rim, which is sometimes difficult to visualize clearly by TEE. A previous study showed that inferior rim deficiency was a significant factor associated with unsuccessful transcatheter closure.[30] Therefore, the additional right parasternal view can contribute to appropriate patient selection and the prediction of procedural results for transcatheter ASD closure.

Considerable experience and operator skills are necessary for evaluating ASD morphology precisely using 2D TTE, equivalent to 2D TEE. There are some issues of technique and some pitfalls. The ultrasound beam should be passed as perpendicularly to the interatrial septum as possible. In addition, gain adjustment using time-gain compensation, focus position, and the use of zoom mode (high frame rate) should be set for morphologic evaluation. In addition, control of respiration and body position should be required to avoid potential artifacts such as dropout and side lobe.

Three-Dimensional Echocardiography Using the Right Parasternal Approach

ASDs are known to have complex geometry that may be elliptical, ovoid, or multiple defects or fenestrations.[20,21] Three-dimensional echocardiography provides more spatial anatomic information without the need for mental 2D reconstruction. There have been several studies on the usefulness for assessing ASDs of 3D transesophageal echocardiographic reconstruction[10-12] and real-time 3D TEE.[18-21] In addition, some previous studies have demonstrated possible usefulness of 3D TTE for evaluating ASD morphology.[18,21,22] Acar *et al.*[31] reported a high correlation between 3D transthoracic and 3D transesophageal echocardiographic measurements of maximal ASD diameter in pediatric patients. Van den Bosch *et al.*[13] demonstrated that real-time 3D TTE enabled reliable assessment of the dimensions of ASDs and the exact location and extent of the surrounding rim, and they reported an excellent correlation of real-time 3D transthoracic echocardiographic findings compared with surgical and 2D transesophageal echocardiographic measurements of ASDs in pediatric and relatively young adult patients. Chen *et al.*[14] reported that 3D TTE could provide accurate diagnosis of sinus venosus ASDs. In terms of the usefulness of 3D TTE in the right parasternal approach for evaluating ASD morphology, although there was one case report, studies with a sufficient number patients and including patients with a wide age range have been limited. In the present study, we demonstrated that the use of the right parasternal approach in addition to the conventional left approach improved the feasibility of visualization of satisfactory 3D images, even in adult patients.

Limitations

This study had some limitations. First, the number of patients in this study was relatively small to conclude whether the extent of variation in ASD type was taken into account. Second, almost all patients in the present study were referred from other hospitals to our institution for transcatheter closure of ASDs. Therefore, patient selection bias could have existed before enrollment. Third, visualizing ASDs and surrounding rims using the right parasternal approach requires a learning curve. In this study, interobserver variability and intraobserver variability were quantitatively evaluated by two skilled operators. Finally, evaluation in the subcostal view may improve the feasibility and accuracy of TTE.

CONCLUSIONS

The use of the right parasternal approach enables detailed morphologic evaluation, especially for longitudinal ASD diameter, superoanterior rim diameter, and inferoposterior rim diameter of ASDs in a longitudinal vena cava superior-inferior plane of the interatrial septum. In patients with suboptimal images with the conventional left approach, additional 3D TTE in the right parasternal approach can improve the feasibility of obtaining optimal 3D images to evaluate the shapes and locations of ASDs.

REFERENCES

1. Butera G, Romagnoli E, Carminati M, Chessa M, Piazza L, Negura D, et al. Treatment of isolated secundum atrial septal defects: impact of age and defect morphology in 1,013 consecutive patients. Am Heart J 2008;156:706-12.
2. Chessa M, Carminati M, Butera G, Bini RM, Drago M, Rosti L, et al. Early and late complications associated with transcatheter occlusion of secundum atrial septal defect. J Am Coll Cardiol 2002;39:1061-5.
3. Berger F, Ewert P, Björnstad PG, Dähnert I, Krings G, Brilla-Austenat I, et al. Transcatheter closure as standard treatment for most interatrial defects: experience in 200 patients treated with the Amplatzer Septal Occluder. Cardiol Young 1999;9:468-73.
4. Du ZD, Hijazi ZM, Kleinman CS, Silverman NH, Larntz K. Amplatzer nvestigators. Comparison between transcatheter and surgical closure of secundum atrial septal defect in children and adults: results of a multicenter nonrandomized trial. J Am Coll Cardiol 2002;39:1836-44.
5. Thomson JD, Aburawi EH, Watterson KG, Van Doorn C, Gibbs JL. Surgical and transcatheter (Amplatzer) closure of atrial septal defects: a prospective comparison of results and cost. Heart 2002;87:466-9.
6. Hanrath P, Schlüter M, Langenstein BA, Polster J, Engel S, Kremer P, et al. Detection of ostium secundum atrial septal defects by transoesophageal cross-sectional echocardiography. Br Heart J 1983;49:350-8.
7. Morimoto K, Matsuzaki M, Tohma Y, Ono S, Tanaka N, Michishige H, et al. Diagnosis and quantitative evaluation of secundum-type atrial septal defect by transesophageal Doppler echocardiography. Am J Cardiol 1990;66:85-91.
8. Kronzon I, Tunick PA, Freedberg RS, Trehan N, Rosenzweig BP, Schwinger ME. Transesophageal echocardiography is superior to

transthoracic echocardiography in the diagnosis of sinus venosus atrial septal defect. J Am Coll Cardiol 1991;17:537-42.
9. Mehta RH, Helmcke F, Nanda NC, Pinheiro L, Samdarshi TE, Shah VK. Uses and limitations of transthoracic echocardiography in the assessment of atrial septal defect in the adult. Am J Cardiol 1991;67:288-94.
10. Tamborini G, Pepi M, Susini F, Trabattoni D, Maltagliati A, Berna G, et al. Comparison of two- and three-dimensional transesophageal echocardiography in patients undergoing atrial septal closure with the Amplatzer Septal Occluder. Am J Cardiol 2002;90:1025-8.
11. Pepi M, Tamborini G, Bartorelli AL, Trabattoni D, Maltagliati A, De Vita S, et al. Usefulness of three-dimensional echocardiographic reconstruction of the Amplatzer Septal Occluder in patients undergoing atrial septal closure. Am J Cardiol 2004;94:1343-7.
12. Acar P, Saliba Z, Bonhoeffer P, Aggoun Y, Bonnet D, Sidi D, et al. Influence of atrial septal defect anatomy in patient selection and assessment of closure with the Cardioseal device; a three-dimensional transoesophageal echocardiographic reconstruction. Eur Heart J 2000;21:573-81.
13. Van den Bosch AE, Ten Harkel DJ, McGhie JS, Roos-Hesselink JW, Simoons ML, Bogers AJ, et al. Characterization of atrial septal defect assessed by real-time 3-dimensional echocardiography. J Am Soc Echocardiogr 2006;19:815-21.
14. Chen CA, Wang JK, Hsu JY, Hsu HH, Chen SJ, Wu MH. Diagnosis of inferior sinus venosus atrial septal defects using transthoracic three-dimensional echocardiography. J Am Soc Echocardiogr 2009;23:457.e4-6.
15. Mehmood F, Vengala S, Nanda NC, Dod HS, Sinha A, Miller AP, et al. Usefulness of live three-dimensional transthoracic echocardiography in the characterization of atrial septal defects in adults. Echocardiography 2004;21:707-13.
16. Mazic U, Gavora P, Masura J. The role of transesophageal echocardiography in transcatheter closure of secundum atrial septal defects by the Amplatzer Septal Occluder. Am Heart J 2001;142:482-8.
17. Prokselj K, Kozelj M, Zadnik V, Podnar T. Echocardiographic characteristics of secundum-type atrial septal defects in adult patients: implications for percutaneous closure using Amplatzer Septal Occluders. J Am Soc Echocardiogr 2004;17:1167-72.
18. Taniguchi M, Akagi T, Watanabe N, Okamoto Y, Nakagawa K, Kijima Y, et al. Application of real-time three-dimensional transesophageal echocardiography using a matrix array probe for transcatheter closure of atrial septal defect. J Am Soc Echocardiogr 2009;22:1114-20.
19. Kijima Y, Taniguchi M, Akagi T, Nakagawa K, Kusano K, Ito H, et al. Torn atrial septum during transcatheter closure of atrial septal defect visualized by real-time three-dimensional transesophageal echocardiography. J Am Soc Echocardiogr 2010;23:1222.e5-8.
20. Lodato JA, Cao QL, Weinert L, Sugeng L, Lopez J, Lang RM, et al. Feasibility of real-time three-dimensional transoesophageal echocardiography for guidance of percutaneous atrial septal defect closure. Eur J Echocardiogr 2009;10:543-8.
21. Johri AM, Witzke C, Solis J, Palacios IF, Inglessis I, Picard MH, et al. Real-time three-dimensional transesophageal echocardiography in patients with secundum atrial septal defects: outcomes following transcatheter closure. J Am Soc Echocardiogr 2011;24:431-7.
22. Tei C, Tanaka H, Kashima T, Yoshimura H, Minagoe S, Kanehisa T. Real-time cross-sectional echocardiographic evaluation of the interatrial septum by right atrium-interatrial septum-left atrium direction of ultrasound beam. Circulation 1979;60:539-46.
23. Minagoe S, Tei C, Kisanuki A, Arikawa K, Nakazono Y, Yoshimura H, et al. Noninvasive pulsed Doppler echocardiographic detection of the direction of shunt flow in patients with atrial septal defect: usefulness of the right parasternal approach. Circulation 1985;71:745-53.
24. McDonald RW, Rice MJ, Reller MD, Marcella CP, Sahn DJ. Echocardiographic imaging techniques with subcostal and right parasternal longitudinal views in detecting sinus venosus atrial septal defects. J Am Soc Echocardiogr 1996;9:195-8.
25. Iliceto S, Antonelli G, Sorino M, Ricci A. Detection of atrial septal defect by right sternal border echocardiography. Am J Cardiol 1984;54:376-8.
26. Luckie M, Buckley H, Khattar R. Echocardiographic detection of atrial septal defects: the forgotten view. Echocardiography 2010;27:97-9.
27. Rudski LG, Lai WW, Afilalo J, Hua L, Handschumacher MD, Chandrasekaran K, et al. Guidelines for the echocardiographic assessment of the right heart in adults: a report from the American Society of Echocardiography endorsed by the European Association of Echocardiography, a registered branch of the European Society of Cardiology, and the Canadian Society of Echocardiography. J Am Soc Echocardiogr 2010;23:685-713.
28. Shub C, Dimopoulos IN, Seward JB, Callahan JA, Tancredi RG, Schattenberg TT, et al. Sensitivity of two-dimensional echocardiography in the direct visualization of atrial septal defect utilizing the subcostal approach: experience with 154 patients. J Am Coll Cardiol 1983;2:127-35.
29. Konstantinides S, Kasper W, Geibel A, Hofmann T, Köster W, Just H. Detection of left-to-right shunt in atrial septal defect by negative contrast echocardiography: a comparison of transthoracic and transesophageal approach. Am Heart J 1993;126:909-17.
30. Varma C, Benson LN, Silversides C, Yip J, Warr MR, Webb G, et al. Outcomes and alternative techniques for device closure of the large secundum atrial septal defect. Catheter Cardiovasc Interv 2004;61:131-9.
31. Acar P, Dulac Y, Roux D, Rougé P, Duterque D, Aggoun Y. Comparison of transthoracic and transesophageal three-dimensional echocardiography for assessment of atrial septal defect diameter in children. Am J Cardiol 2003;91:500-2.

Circulation
Cardiovascular Interventions
JOURNAL OF THE AMERICAN HEART ASSOCIATION
American Heart Association
Learn and Live

Refined Balloon Pulmonary Angioplasty for Inoperable Patients with Chronic Thromboembolic Pulmonary Hypertension

Hiroki Mizoguchi, Aiko Ogawa, Mitsuru Munemasa, Hiroshi Mikouchi, Hiroshi Ito and Hiromi Matsubara

Circ Cardiovasc Interv 2012;5;748-755; originally published online November 27, 2012;
DOI: 10.1161/CIRCINTERVENTIONS.112.971077
Circulation: Cardiovascular Interventions is published by the American Heart Association. 7272 Greenville Avenue, Dallas, TX 72514
Copyright © 2012 American Heart Association. All rights reserved. Print ISSN: 1941-7640. Online ISSN: 1941-7632

The online version of this article, along with updated information and services, is located on the World Wide Web at:
http://circinterventions.ahajournals.org/content/5/6/748.full

Data Supplement (unedited) at:
http://circinterventions.ahajournals.org/content/suppl/2012/11/27/CIRCINTERVENTIONS.112.971077.DC1.html

Subscriptions: Information about subscribing to Circulation: Cardiovascular Interventions is online at http://circinterventions.ahajournals.org/site/subscriptions/

Permissions: Permissions & Rights Desk, Lippincott Williams & Wilkins, a division of Wolters Kluwer Health, 351 West Camden Street, Baltimore, MD 21201-2436. Phone: 410-528-4050. Fax: 410-528-8550. E-mail: journalpermissions@lww.com

Reprints: Information about reprints can be found online at http://www.lww.com/reprints

Downloaded from circinterventions.ahajournals.org at OKA-DAI FUZOKU TOSHOKAN SHIKAT on May 12, 2013

Refined Balloon Pulmonary Angioplasty for Inoperable Patients with Chronic Thromboembolic Pulmonary Hypertension

Hiroki Mizoguchi, MD; Aiko Ogawa, MD, PhD; Mitsuru Munemasa, MD, PhD; Hiroshi Mikouchi, MD, PhD; Hiroshi Ito, MD, PhD; Hiromi Matsubara, MD, PhD

Background—Although balloon pulmonary angioplasty (BPA) for inoperable patients with chronic thromboembolic pulmonary hypertension was first reported over a decade ago, its clinical application has been restricted because of limited efficacy and complications. We have refined the procedure of BPA to maximize its clinical efficacy.

Methods and Results—Sixty-eight consecutive patients with inoperable chronic thromboembolic pulmonary hypertension underwent BPA. We evaluated pulmonary artery diameters and determined the appropriate balloon size by using intravascular ultrasound. We performed BPA in a staged fashion over multiple, separate procedures to maximize efficacy and reduce the risk of reperfusion pulmonary injury. A total of 4 (2–8) sessions were performed in each patient, and the number of vessels dilated per session was 3 (1–14). The World Health Organization functional class improved from 3 to 2 ($P<0.01$), and mean pulmonary arterial pressure was decreased from 45.4±9.6 to 24.0±6.4 mm Hg ($P<0.01$). One patient died because of right heart failure 28 days after BPA. During follow-up for 2.2±1.4 years after the final BPA, another patient died of pneumonia, and the remaining 66 patients are alive. In 57 patients who underwent right heart catheterization at follow-up, improvement of mean pulmonary arterial pressure was maintained (24.0±5.8 mm Hg at 1.0±0.9 years). Forty-one patients (60%) developed reperfusion pulmonary injury after BPA, but mechanical ventilation was required in only 4 patients.

Conclusions—Our refined BPA procedure improves clinical status and hemodynamics of inoperable patients with chronic thromboembolic pulmonary hypertension, with a low mortality. A refined BPA procedure could be considered as a therapeutic approach for patients with inoperable chronic thromboembolic pulmonary hypertension. (***Circ Cardiovasc Interv.* 2012;5:748-755.**)

Key Words: peripheral vascular disease ■ pulmonary hypertension ■ reperfusion ■ revascularization

Patients with chronic thromboembolic pulmonary hypertension (CTEPH) have a poor prognosis. Pulmonary endarterectomy can dramatically reduce pulmonary arterial pressure in selected patients with CTEPH to improve their prognosis.[1] However, not all patients can undergo pulmonary endarterectomy because of technical limitations.[2–4] Pulmonary endarterectomy for CTEPH with peripherally located organized thrombus is associated with less improvement in pulmonary hemodynamics and has a higher mortality in patients compared with those with proximal thrombi.[1] The latest guidelines for the diagnosis and treatment for pulmonary hypertension indicate that the selection of patients for pulmonary endarterectomy depends on the extent and location of the organized thrombi in relation to the degree of pulmonary hypertension and taking into consideration age and comorbidities.[5]

Editorial see p 744

Balloon pulmonary angioplasty (BPA) for a patient with CTEPH was first reported in 1988.[6] In 2001, Feinstein et al[7] reported the efficacy of BPA for a series of patients with CTEPH. Although this report showed a significant improvement in hemodynamics and exercise tolerance, these improvements were not as good as those of pulmonary endarterectomy. Moreover, 1 of 18 patients died from reperfusion pulmonary injury and right ventricular failure after BPA. The mortality rate of BPA is not superior to that of pulmonary endarterectomy. Pulmonary endarterectomy is an established treatment for CTEPH and the mortality rate was recently reported to be as low as 2.2%,[8] although it varies up to 14.3% depending on the institute.[9–11] More than 20 years after the first report of BPA, BPA is still not widely accepted as a therapeutic option for inoperable patients with CTEPH.

Received March 30, 2012; accepted October 30, 2012.

From the Division of Cardiology (H.Miz., M.M., H.Mik., H.Mat.) and Department of Clinical Science (A.O., H.Mat.), National Hospital Organization Okayama Medical Center, Okayama, Japan; Department of Cardiovascular Medicine, Okayama University Graduate School of Medicine, Dentistry and Pharmaceutical Sciences, Okayama, Japan (H.I.).

The online-only Data Supplement is available at http://circinterventions.ahajournals.org/lookup/suppl/doi:10.1161/CIRCINTERVENTIONS.112.971077/-/DC1.

Correspondence to Hiromi Matsubara, MD, PhD, Division of Cardiology and Department of Clinical Science, National Hospital Organization Okayama Medical Center, 1711-1 Tamasu, Kita-ku, Okayama 701–1192, Japan. E-mail matsubara.hiromi@gmail.com

© 2012 American Heart Association, Inc.

Circ Cardiovasc Interv **is available at http://circinterventions.ahajournals.org** **DOI: 10.1161/CIRCINTERVENTIONS.112.971077**

Downloaded from circinterventions.ahajournals.org at OKADAI FUZOKU TOSHOKAN SHIKAT on May 12, 2013

WHAT IS KNOWN

- The efficacy of balloon pulmonary angioplasty (BPA) was previously reported in a small series of inoperable patients with chronic thromboembolic pulmonary hypertension, who have a poor prognosis.
- However, BPA has not been widely adopted owing to relatively less improvement and higher mortality compared with surgical pulmonary endarterectomy.

WHAT THE STUDY ADDS

- We have refined the procedure of BPA by using intravascular ultrasound to provide more accurate estimates of the diameters of target pulmonary arteries.
- We performed BPA in a staged fashion over multiple procedures to reduce the risk of pulmonary reperfusion injury while still achieving an effective therapeutic result.
- Although there is a learning curve in performing this procedure, our refined approach to BPA may be a treatment option for patients with inoperable chronic thromboembolic pulmonary hypertension.

We have recognized 2 major problems that need to be resolved for improving the clinical efficacy of BPA. One problem is insufficient improvement in hemodynamics after the BPA procedure, and the other is the high incidence of potentially fatal complications, including reperfusion pulmonary injury and rupture of the pulmonary artery. We have refined the BPA procedure to improve its clinical efficacy. The major difference of our refined BPA procedure is the introduction of intravascular ultrasound (IVUS) to determine the optimal balloon size. IVUS has enabled us to determine the actual size of the target lesions, which leads to improved hemodynamic outcome and reduced risk of reperfusion pulmonary injury and rupture of the pulmonary artery. We studied the clinical efficacy of this refined BPA procedure with advanced care for inoperable patients with CTEPH.

Methods

Patient Selection

Sixty-eight consecutive patients with inoperable CTEPH who underwent BPA between November 2004 and September 2011 were enrolled in this study. BPA was performed after approval of the Institutional Review Board, and written informed consent was obtained from each patient before the procedure. A diagnosis of CTEPH was based on detailed medical history, a physical examination, chest radiography, a chest computed tomography (CT) scan, transthoracic echocardiography, lung ventilation-perfusion scintigraphy, right heart catheterization, and angiographic demonstration of multiple stenoses and obstruction of bilateral pulmonary arteries. Pulmonary angiography showed at least 1 of the following features: pouching defects; webs or bands, intimal irregularities, abrupt vascular narrowing, and complete vascular obstruction.[12] All patients were diagnosed as inoperable by experienced surgeons because of the location of thrombi and surgical accessibility, age, and comorbidities. All patients were in World Health Organization (WHO) functional class III or IV despite medical treatment. None of the patients were excluded from undergoing BPA based on age restrictions or severity of hemodynamics.

Management Before BPA

All patients were administered epoprostenol to decrease pulmonary arterial pressure as much as possible. Epoprostenol was started at 1 ng/kg/min ≈5 days before the procedure and increased by 1 ng/kg/min each day to a maximum of 5 ng/kg/min by the day of BPA. If a patient was already on long-term epoprostenol therapy before BPA, the dosage was unchanged. All medications, including warfarin, were maintained, except for beraprost sodium, which was discontinued when the dosage of epoprostenol reached 2 ng/kg/min. If the cardiac index was <2.2 L/min/m^2, dobutamine at a dose of 2 to 3 μg/kg/min was administered before the procedure.

BPA Procedure

On the basis of the results of pulmonary angiography and perfusion scintigraphy, we selected in advance which branches of the pulmonary arteries to dilate. We targeted webs (Figure 1) or bands, abrupt vascular narrowing, or complete vascular obstruction (Figure 2). The lower lobe was targeted for the initial BPA in most cases. Targeted vessels were limited within 2 vessels in a single lobe of the lung in the initial BPA session to avoid the occurrence of severe reperfusion pulmonary injury. We placed a 9F indwelling sheath (Arrow-Flex; Teleflex, Durham, NC) into a vein (mainly into the internal jugular vein [n=65] and occasionally into the subclavian [n=1] or femoral vein [n=2]) and brought a 6F long sheath (Bright Tip Sheath Introducer; Cordis/Johnson & Johnson, New Brunswick, NJ) to the main pulmonary artery via the 9F sheath, using 0.035-inch wire (Radifocus Guide Wire M; Terumo, Tokyo, Japan). Heparin (5000 U) was administered when the sheath was inserted, and 1000 U of heparin was added every hour during the procedure. We selected a branch of the pulmonary artery by a 6F guiding catheter (Mach 1 peripheral MP; Boston Scientific, Natick, MA) and performed angiography (Figure 1A and 1B). We crossed a 0.014-inch wire (Cruise; Asahi Intecc, Tokyo, Japan) to the targeted lesion and evaluated the lumen size of the vessel with IVUS (Eagle Eye Platinum; Volcano, San Diego, CA) (Figure 1C). Because organized thrombi are isoechoic, we used ChromaFlo (Volcano, San Diego, CA) computer software to clearly visualize and distinguish lumen and thrombi. We measured the vessel diameter at the site where thrombi occupied the lumen and the vessel was most severely stenosed. After determination of the vessel diameter with IVUS, we usually used a 2-mm balloon for the initial dilatation to avoid rupture and dissection of the pulmonary artery. We dilated the vessel by balloon catheters of appropriate size (2 to 4 mm, IKAZUCHI PAD, Kaneka, Osaka, Japan; 5 to 7 mm, Bandicoot RX, St. Jude Medical, St. Paul, MN and Aviator Plus, Cordis/Johnson & Johnson, New Brunswick, NJ; 8 mm, Sterling Monorail, Boston Scientific, Natick, MA). The appropriate size was determined according to the vessel diameter measured by IVUS. The maximal size was set not to >90% of the original size of the vessel diameter, considering tapering and shrinkage of pulmonary arteries owing to reduced flow before BPA. The balloon was inflated by hand until the indentation disappeared or until the balloon was fully expanded. After inflation, angiography and IVUS were performed to ascertain that the vessel was dilated sufficiently and did not rupture (Figure 1D, 1E, and 1F). Dilatation was repeated if it was not sufficient by evaluation with IVUS, pulmonary arterial flow did not improve angiographically, or the pressure gradient across the dilated site >10 mm Hg. The procedure was discontinued when oxygen desaturation was >4% or hemo sputum occurred.

In the following sessions, targeted vessels were also limited within a unilateral lung, until the mean pulmonary arterial pressure was decreased to <35 mm Hg. When mean pulmonary arterial pressure was <35 mm Hg, BPA could be performed in both lungs in 1 session. BPA was repeated at an interval of 5 to 14 days after the initial procedure. Additional BPA at an interval of 12 to 16 weeks after the procedure was recommended until mean pulmonary arterial pressure at the end of hemodynamic monitoring became <30 mm Hg.

Downloaded from circinterventions.ahajournals.org at OKA-DAI FUZOKU TOSHOKAN SHIKAT on May 12, 2013

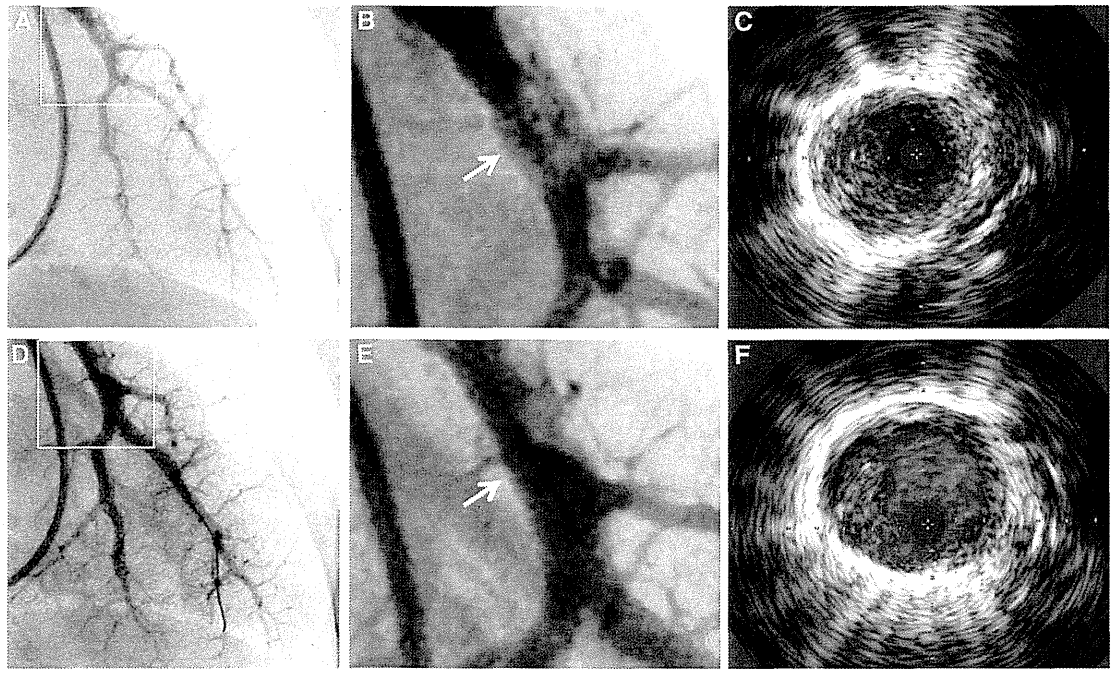

Figure 1. Representative angiographic and intravascular ultrasound (IVUS) images of balloon pulmonary angioplasty (BPA). **A**, Site of an intravascular web of the left pulmonary artery is indicated with a **square** on the angiogram. Peripheral arteries have shrunk because of a reduction in blood flow. **B**, A magnified image of a square in Figure 1A. An intravascular web is indicated with **arrows**. **C,** IVUS image (at the arrow in Figure 1B) shows organized thrombi, which occupy the lumen, and blood flow is limited in small channels. **D**, After a 5-mm balloon is dilated at 8 atm, an angiogram shows a dilated vessel and increased flow in the distal arteries after BPA. **E**, A magnified image of an intravascular web shown in Figure 1D. An intravascular web indicated with **arrows** is compressed and a vessel diameter of the distal artery is increased. **F**, IVUS image (at the arrow in Figure 1E). Thrombi are forced to 1 side and the lumen size is enlarged.

Management After BPA

We used noninvasive positive airway pressure ventilation at least 24 hours after BPA. Hemodynamics were continuously monitored with a Swan-Ganz catheter (Swan-Ganz CCOmbo V; Edwards Lifesciences, Irvine, CA) after the BPA procedure until noninvasive positive airway pressure ventilation could be weaned off. We performed a chest X-ray immediately after patients returned to the Cardiac Care Unit and performed a CT scan within 4 hours after BPA to check for increased density of the dilated segments. Epoprostenol and dobutamine were discontinued 3 days after a series of BPAs. Methylprednisolone (500 mg/day) was administered for 3 days to reduce reperfusion pulmonary injury after BPA.

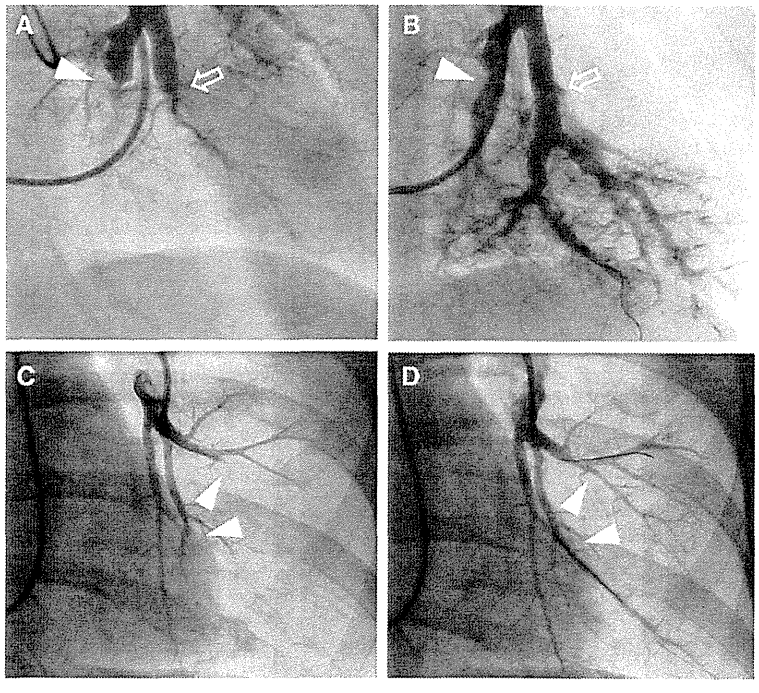

Figure 2. Representative pulmonary angiograms before and after balloon pulmonary angioplasty (BPA). **A**, Pulmonary angiogram shows abrupt vascular narrowing (**arrow**) and complete vascular obstruction (**arrowhead**) in the left lower arteries before BPA. **B**, After dilatation of target arteries with a 6-mm balloon at 6 atm, the lesions are successfully opened. **C**, Pulmonary angiogram shows complete vascular obstruction (**arrowhead**) in the left lower arteries before BPA. **D**, After dilatation of target arteries with a 2-mm balloon at 8 atm, the lesions are successfully opened.

Downloaded from circinterventions.ahajournals.org at OKA-DAI FUZOKU TOSHOKAN SHIKAT on May 12, 2013

Clinical Outcomes

Patients were followed up at least every 6 months after the final BPA. The effectiveness of BPA was evaluated by improvement of WHO functional class, hemodynamic parameters (systolic, diastolic and mean pulmonary arterial pressure, cardiac index, and pulmonary vascular resistance), plasma levels of brain natriuretic peptide, and 6-minute walk distance before the first session of BPA, immediately after the final session of BPA, and at follow-up.

Statistical Analysis

Results are expressed as the mean±SD. Integers, including the number of sessions and balloons, are expressed as the median and range. Differences between variables measured at baseline and after BPA were tested by the paired *t* test. WHO functional class is expressed as the median and number of patients in each class, and changes in WHO functional class were evaluated using the Wilcoxon signed rank test. For assessing the difference among before, immediately after, and follow-up data, variables were analyzed by linear mixed modeling. Generalized linear mixed modeling was used to determine the learning curve for BPA, the incidence of complications between the initial 128 sessions (performed between November 2004 and October 2010), and the recent 127 sessions (performed between November 2010 and September 2011). All analyses were performed with IBM SPSS Statistics 20 (IBM, Armonk, NY). Statistical significance was defined as $P<0.05$.

Results

Baseline Characteristics

Our study included 53 females (78%) and 15 males (22%) with inoperable CTEPH. The mean age was 62.2±11.9 years old, with a range of 38 to 82-years old at the time of first admission. Disease duration (the time between diagnosis and the first admission to our hospital) was 3.2±3.2 years. Baseline patient characteristics are shown in Table 1. All patients were in WHO functional class III or IV with a high pulmonary arterial pressure. All patients were treated with warfarin, supplemental oxygen therapy, and >1 pulmonary hypertension-targeted drug. In addition, 5 patients were transferred to our hospital with intravenous infusion of dobutamine because of severe right heart failure.

Table 1. Clinical and Hemodynamic Data Before and After BPA

	Before BPA (n=68)	After BPA (n=67)	*P* Value
WHO functional class (I/II/III/IV)	3 (0/0/49/19)	2 (11/53/3/0)	<0.01
Oxygen inhalation (L/min)	3.0±1.4	1.3±1.0	<0.01
6MWD, m	296±108	368±83	<0.01
BNP, pg/mL	330±444	35±55	<0.01
sPAP, mm Hg	81.3±16.9	42.3±11.9	<0.01
dPAP, mm Hg	24.3±7.1	13.4±4.8	<0.01
mPAP, mm Hg	45.4±9.6	24.0±6.4	<0.01
RAP, mm Hg	8.1±4.4	1.9±1.5	<0.01
CI, L/min/m^2	2.2±0.7	3.2±0.6	<0.01
PVR, dyne sec/cm^5	942±367	327±151	<0.01

Values other than WHO functional class are expressed as mean±SD. WHO functional class is presented as the median and number of patients in each class.

6MWD indicates 6-minute walk distance; BPA, balloon pulmonary angioplasty; BNP, brain natriuretic peptide; CI, cardiac index; dPAP, diastolic pulmonary arterial pressure; mPAP, mean pulmonary arterial pressure; PVR, pulmonary vascular resistance; RAP, right atrial pressure; sPAP, systolic pulmonary arterial pressure; and WHO, world health organization.

BPA Procedure

The 68 patients underwent a total of 255 BPA sessions. A total of 4 (2–8) sessions were performed in each patient, and the number of vessels dilated per session was 3 (1–14). Preoperative application of epoprostenol only resulted in a slight decrease in mean pulmonary arterial pressure (to 42.3±8.1 mm Hg, $P<0.05$). After observation using IVUS and Chroma-Flo, balloons matched to the vessel diameters were selected. As a result, we used 3 (1–6) balloons in 1 session, and the number of different balloon sizes per vessel was 2 (1–3). Contrast medium of 160.2±57.2 mL/session was required. Patients underwent 2 (1–6) sessions during 1 admission. The percentages of targeted arteries in 150 arteries at the initial session and in 558 arteries in the total sessions are shown in Table 2. At the initial BPA, the lower lobe of a unilateral lung was the target in most cases and none of the arteries in the left upper lobe were targeted. Ultimately, BPA was performed in all segments and there were no inaccessible lesions. The relative reductions in mean pulmonary arterial pressure and absolute change in mean pulmonary arterial pressure were correlated with the number of segments of pulmonary arteries treated by BPA (Figure 3).

Outcomes of BPA

The changes in clinical parameters before and after BPA (within 1 week after the final session of BPA) are summarized in Table 1 and Figure 4. One patient died 28 days after the third session of BPA because of right-sided heart failure, who had been transferred from another hospital after 3 months of hospitalization because of dobutamine-dependent severe right heart failure. After BPA, severe reperfusion pulmonary injury developed and subsequent worsening of right-sided heart failure required percutaneous cardiopulmonary support, which could not be recovered. Among the other 67 patients, 64 patients (96%) were in WHO functional class I or II after BPA, while there were no patients in classes I

Table 2. Distribution of Dilated Pulmonary Arteries at the Initial and Total Sessions

Right Lung Segment	Initial n (%)	Total n (%)	Left Lung Segment	Initial n (%)	Total n (%)
A1	1 (0.7)	44 (7.9)	A1+2	0 (0.0)	32 (5.7)
A2	2 (1.3)	40 (7.2)			
A3	1 (0.7)	32 (5.7)	A3	0 (0.0)	14 (2.5)
A4	3 (2.0)	27 (4.8)	A4	0 (0.0)	2 (0.4)
A5	8 (5.3)	30 (5.4)	A5	0 (0.0)	3 (0.5)
A6	2 (1.3)	6 (1.1)	A6	0 (0.0)	17 (3.0)
A7	13 (8.7)	30 (5.4)			
A8	32 (21.3)	48 (8.6)	A8	3 (2.0)	36 (6.5)
A9	33 (22.0)	48 (8.6)	A9	8 (5.3)	54 (9.7)
A10	40 (26.7)	54 (9.7)	A10	4 (2.7)	41 (7.3)

Initial indicates absolute number and percentage of targeted arteries in 150 arteries at the initial session; and total, absolute number and percentage of targeted arteries in 558 arteries in the total sessions.

Downloaded from circinterventions.ahajournals.org at OKA-DAI FUZOKU TOSHOKAN SHIKAT on May 12, 2013